Ribo-tag translatomic profiling of *Drosophila* oenocyte reveals down-regulation of peroxisome and mitochondria biogenesis under aging and oxidative stress

Kerui Huang[1]*, Wenhao Chen[2], Hua Bai[1]*

1 Department of Genetics, Development, and Cell Biology, Iowa State University, Ames, IA 50011, USA

2 Department of Electrical and Computer Engineering, Iowa State University, Ames, IA 50011, USA

***Corresponding Authors:**

Kerui Huang

Phone: 515-294-3842

Email: keruih@iastate.edu

Hua Bai

Phone: 515-294-9395

Email: hbai@iastate.edu

Running title:

***Drosophila* oenocyte Ribo-tag profiling**

Abstract

Background: Reactive oxygen species (ROS) has been well established as toxic, owing to its direct damage on genetic materials, protein and lipids. ROS is not only tightly associated with chronic inflammation and tissue aging but also regulates cell proliferation and cell signaling. Yet critical questions remain in the field, such as detailed genome-environment interaction on aging regulation, and how ROS and chronic inflammation alter genome that leads to aging. Here we used cell-type-specific ribosome profiling (Ribo-tag) to study the impacts of aging and oxidative stress on the expression of actively translated mRNA in *Drosophila* oenocytes, a specialized hepatocyte-like cells and an understudied insect tissue.

Results: Through ribosome profiling, we obtain oenocyte translatome, from which we identify genes specifically expressed in adult oenocyte. Many of them are cuticular proteins, including tweedle family proteins, which are critical for structural constituent of cuticle. Oenocytes are enriched with genes involved in unsaturated fatty acids, ketone body synthesis and degradation, and xenobiotics. Aging and paraquat exhibit distinct regulation on oenocyte translatome. 3411 genes are differentially regulated under aging, only 1053 genes under paraquat treatment. Gene set enrichment analysis identify pathways with overall declined expression under aging and paraquat treatment, especially peroxisome, mitochondrial function and metabolic pathways. In comparing to human liver-elevated proteins, we identify orthologues specifically enriched in oenocyte. Those orthologues are involved in liver ketogenesis, ethanol metabolism, and glucose metabolism. Gene Ontology (GO) analysis shows different functions between oenocyte and fat body, which is another widely accepted model for liver in *Drosophila*. Lastly, 996 genes are regulated to paraquat stress in young age, however in aged flies, the number decreased to 385. Different sets of genes are regulated in response to stress between young and old flies.

Conclusions: Our analysis reveals 17 oenocyte specific genes, which help to define oenocyte's function. Oenocyte shares some aspects of human liver function, makes the oenocytes applicable as a model system. Our gene set analysis provides insight into fundamental changes of oenocyte under aging and oxidative stress. The finding that peroxisome is down-regulated under oxidative stress suggests peroxisome plays important role in regulating oenocyte homeostasis under aging, which can have a significant impact on whole body and fat metabolism.

Keywords: oxidative stress, aging, oenocyte, hepatocyte-like cells, ribosomal profiling, mitochondria ribosomal proteins, peroxisome

Introduction

Oenocyte

Oenocytes are secretory cells that are found in most pterygote insects [1]. Oenocyte is important for growth, because oenocyte ablation will trigger growth arrest and lethality before reaching pupariation [2]. Several studies have attempted to decipher oenocyte's function on transcriptional level. Studies have shown that 51 transcripts are enriched in larvae oenocytes, and 22 of them have human homologues that are fat-metabolizing genes expressed in hepatocytes [2]. Chatterjee et al., 2014 conducted tissue-specific expression profiling on oenocyte, confirming its role on lipid mobilization during fasting. Transcriptome of oenocytes from *Aedes aegypti* pupae reveals that oenocyte highly expresses transcripts from cytochrome P450 superfamily, whose members are crucial for detoxification and lipid metabolism [3]. Despite the importance of oenocyte, a comprehensive understanding on *Drosophila* adult oenocyte function is still lacking, mainly due to the challenge for obtaining samples without contamination.

Hall marks of aging and Oxidative stress

Aging has been characterized as gradual decline of cell physiological integrity and maintenance, leading to cell death and vulnerability to diseases. The topic has embarked extensive research and investigation. Recently molecular and cellular hallmarks of aging have been identified. The nine hallmarks are considered to contribute to aging process and lead to the aging phenotypes. Amelioration of these processes can retard normal aging process and increase lifespan. The nine hallmarks are: 1) genomic instability, because of DNA damaged by endogenous and exogenous threats, including reactive oxygen species (ROS). 2) Telomere attribution. 3) Epigenetic alterations involve modification of histones, DNA methylation and chromatin remodeling. 4) Loss of proteostasis involves inability to stabilize folded proteins through chaperone, and failure of protein degradation by lysosome or proteasome. 5) Dysregulated nutrient sensing, including insulin signaling pathway, nutrient-sensing systems. 6) Mitochondrial dysfunction with aging results in increased production of ROS, which can cause further mitochondrial damage and cellular damage. 7) Cellular senescence. 8) stem cell exhaustion. 9) Altered intercellular communication [4].

Liver aging

Aging is the major risk factor for chronic liver diseases. Studies have found that aging is associated with alterations of hepatic structure, function as well as changes in liver cells. For

example, the volume and blood flow of liver decreases with aging, diminished regenerative ability, as well as declines in the Phase I metabolism of certain drugs. The blood cholesterol, neutral fat levels and high-density lipoprotein cholesterol increases with time, which will eventually lead to non-alcoholic fatty liver disease (NAFLD). The metabolism for low-density lipoprotein cholesterol decreases by 35% [5]. Aging leads to be polyploidy nuclei, decreased area of smooth endoplasmic reticulum, which reduce the synthesis of microsomal proteins in the liver and dysfunction of mitochondria [6]. Aging alters stress-induced expression of heme oxygenase-1, which may lead to lower stress tolerance and sensitivity [7]. In addition, a recent study indicated that age-associated change on CCAAT/enhancer-binding protein (C/EBP) protein family caused liver injury after carbon tetrachloride (CCl_4) treatments [8]. They observed altered chromatin structure in old wild type mice and young mice which express an aged-like isoform of C/EBPα. They also found age-related repression on C/EBPα, Farnesoid X Receptor (FXR) and telomere reverse transcriptase [9]. Molecular mechanism for altered liver function during aging include increased ROS formation, DNA damage, activation of p300-C/EBP-dependent neutral fat synthesis [10], a decreased autophagy [11], increased M1 macrophage inflammatory responses [12], and activation of nuclear factor-κB pathways [13,14]. Despite of many advances in detailed genetic control of aging, very little is known about how translatome changes with liver aging and what initiated the aging process.

Oxidative stress generated by imbalanced ROS level could be the key cause for liver damage during aging. Aging is accompanied by increased level of ROS [15], which can damage cellular contents. Paradoxically elevated ROS can act as signaling molecules in maintaining cellular function, a process termed redox biology. Evidence suggests that increasing ROS can promote healthy aging by activating stress-response pathways [16]. The detailed molecular mechanism for redox biology induced pathology or beneficial effect is pressingly needed to solve this paradox. Moreover, what cellular functions changed during liver aging are caused by redox biology is still unknown.

The aim of this study is to establish *Drosophila* oenocyte as a liver model to study its translatome changes under aging. In *Drosophila*, both fat body and oenocytes have been proposed to share similar functions as mammalian liver. In particular, oenocyte exhibit hepatocyte cell-like function for its ability to accumulate lipid droplets (LDs) under fasting, similar to fast-induced fatty liver [2]. Oenocytes are specialized cells in *Drosophila*, which

regulates fat metabolism and is an important site for cuticular hydrocarbon production, pheromone synthesis and detoxification [17,18]. Despite oenocyte performs metabolic functions similar to liver, its specific functions in adult fly physiology and changes under aging is largely unknown. A morphological and cytometric analysis on aged oenocyte was made. They discovered that amounts of cellular components change dramatically because of increased cell size during aging. Aged oenocytes also show an increase of pigmented granules [19]. Tower et al. discovered that cytoplasmic chaperone gene *Hsp70* and the mitochondrial chaperone gene *Hsp22* are upregulated during normal aging in *Drosophila*, specifically in the oenocyte. Their data suggests that mitochondrial malfunction contribute to oenocyte aging [20]. Detailed molecular mechanism for oenocyte aging is still unknown. To establish a liver aging model using *Drosophila* oenocyte, comprehensive study on its protein changes are needed.

Previous analysis on oenocyte primarily focuses on transcription or morphology, instead of translation, which is a more accurate measurement on protein level. In addition, tissue contamination is unavoidable during traditional dissection. Here we utilize RiboTag system originally developed in mouse [21], accompanied by RNA sequencing, to obtain oenocyte-specific ribosome-associated mRNA.

To better understand how oenocyte specifically respond to oxidative stress *in vivo* and how aging changes the genome profile of the tissue, we use ribo-tag and RNA sequencing on ribosome-associated mRNA obtained from oenocyte. Our analysis revealed that aging and paraquat exhibit distinct regulation on oenocyte translatome. Organelle ribosome, proteasome, mitochondrial respiratory chain and rRNA processing are significantly regulated under aging. Whereas paraquat treatment alters translation in fatty acid elongation, fatty acid metabolism, antibacterial humoral response. There is also common translational regulation shared between two processes. Genes involved in oxidoreductase, ribosome structure, peroxisome and fatty acid metabolism are most commonly regulated. Gene set enrichment analysis (GSEA) confirmed that age and paraquat-related decreases in mitochondrial and peroxisomal function and increase in DNA repair. In addition, aged oenocytes show reduced sensitive to paraquat treatment. Our analysis identified 437 oenocyte highly enriched genes and 21 oenocyte unique genes. Finally, our analysis revealed conservation of age-related translational changes between oenocytes and liver.

Results

Characterization of Drosophila oenocytes at adult stage

Oenocytes of *Drosophila* larvae have been shown to accumulate lipid under starvation condition, a process similar to steatosis in mammalian liver [2]. Because there is a dramatic remodeling of oenocytes during the larvae-to-adult transition [1]. It is less clear whether adult oenocytes still maintain the same hepatocyte properties. To address this question, we monitored lipid droplet formation by oil red O staining of starved wild-type adult flies. Consistent with previous studies (cite papers from Gutierrez et al., 2007, and Chatterjee et al., 2014), the number of lipid droplets in adult oenocytes increased significantly upon starvation, suggesting adult oenocytes maintained the hepatocyte-like function (Figure 1A).

Next, we use dihydroethidium (DHE) dye to examine the impacts of aging and oxidative stress on ROS levels of *Drosophila* oenocytes. As shown in Figure 1, both aging and oxidant paraquat (PQ) treatment significantly increased ROS levels in adult oenocytes. Here we only compared two ages, 2 weeks (young) and 4 weeks (middle age). Because we noticed that ROS levels increased at middle age, and previous studies indicate that many genes show differential expression at middle age. Comparing young and middle age will allow us to capture early-onset age-related changes in *Drosophila* oenocytes. Interestingly, young oenocytes showed much higher induction of ROS under 10 mM of PQ treatment than did oenocytes from middle age (Figure 1C). These findings suggest that PQ and aging interact to regulate ROS production in adult oenocytes, and aged oenocytes showed reduced sensitive to PQ treatment. Oenocyte-specific driver PromE-Gal4 was used to drive the expression of FLAG-tagged RpL13A, one of the components of the large ribosomal subunit. To verify the efficiency and specificity of Ribo-tag profiling, we performed a qRT-PCR analysis to measure the expression of a known oenocyte-specific gene *Desaturase 1 (Desat1)*. Desat1 is a transmembrane fatty acid desaturase, its E isoform was found highly expressed in female oenocytes [17]. We found that the expression of *desat1-E* was highly enriched in anti-FLAG immunoprecipitated sample (IP) compared to the input (whole body), suggesting that our Ribo-tag approach can effectively and specially detect the gene expression from female oenocytes. We also set up two control experiments: 1) Immunoprecipitation of oenocyte-specific RpL13A-FLAG expressing females using only magnetic beads without adding FLAG antibody. 2) Immunoprecipitation of control flies without RpL13A-FLAG expression. Average mRNA levels pulled down from the two control groups are

undetectable (Figure 1F), suggesting our Ribo-tag is highly specific to oenocyte, with no or very little contamination from non-specific binding of antibody and magnetic beads.

Differential gene expression (DGE) analysis in oenocyte through Ribo-tag sequencing

Besides its roles in larval development, metabolic homeostasis [22,23], the production of cuticle hydrocarbon [24,25],ecdysteroids[26–29] and elimination of toxic waste products [30–34], oenocyte is poorly characterized during aging and stress. To better understand oenocyte function at molecular level, we performed Ribo-tag profiling to identify the differentially expressed genes in adult oenocytes (Figure 1D).

We performed Ribo-tag sequencing to characterize genome-wide changes of oenocytes translatome (actively translated mRNA profiling) under aging and oxidative stress. Adult flies were aged and sorted into four experimental groups: 1) water fed young female flies that are 2-week-old female flies (water-young); 2) 2-week-old female flies treated with 10 mM of paraquat (paraquat-young); 3) 4-week-old control female flies fed on water (water-aged); 4) 4-week-old female flies treated with 10 mM of paraquat (paraquat-aged). Next-Generation sequencing were performed using Illumina HiSeq 3000. We generated 12 cDNA libraries, single-end, 50 base pair libraries averaged over 4.0 million reads and 7.6X coverage. On average, 82.43% of unique reads are mapped to an annotated the genome using TopHat. An average of 33501263 unique reads were generated per library (Table S1).

We used Cuffdiff to find significant changes in transcript expression between samples. We identified DGEs ($Q < 0.05$ and 2-fold change) under each condition. We compared water-young and paraquat-young flies, 1203 DGEs were found (962 down-regulated and 241 up-regulated). Between water-young and water-aged flies, we found 3578 DGEs (1261 up-regulated and 2317 down-regulated). Between water-aged and paraquat-aged flies, 589 DGEs (336 up-regulated and 253 down-regulated) were identified. Comparing between paraquat-young and paraquat-aged, there are 2120 DGEs (749 up-regulation and 1371 down-regulation).

To eliminate possibility of contamination, we looked at the expression of two epidermis specific enzymes in our dataset. Krotzkopf verkehrt (kkv) is a membrane-inserted glycosyltransferase family 2 chitin synthase that produce polysaccharide chitin. *Kkv* is mainly expressed in epidermis [35], however it has very low expression in oenocyte (0.1 FPKM). In addition, adult cuticle protein 1 (Acp1) specializes in thickening adult cuticle [36]. The protein has high expression in adult carcass (30 FPKM), but it has low expression in the oenocyte (0.2

FPKM). Our profiling data contains low expression for cuticle genes, suggesting that our oenocyte is free of contamination from cuticles.

Aging and paraquat exhibit distinct regulation on oenocyte translatome

To visualize how gene expression varies under different conditions, we performed principal component analysis (PCA) on the fragments per kilobase million (FPKM) reads. The first component accounts for 50% of the variance and the second component accounts for 9% of variance (Figure 2A). The PCA analysis showed that replicates of each condition cluster together, except for one of water-young samples. We also observed that young oenocyte samples were separated well from all aged samples. There was also larger variation between paraquat treatments in young oenocytes, compared with aged oenocytes.

To compare the different impacts on transcriptional changes by aging and paraquat treatment, we performed correlation analysis using FPKM reads from all four groups. The coefficient of determination (R^2) between water-old and water-young groups is 0.861 (Figure 2B); R^2 between water-young and paraquat-young is 0.926 (Figure 2C); R^2 between paraquat-old and water-old is 0.948. Aging induced a bigger transcriptional shift compared to paraquat treatment (Figure 2D). Although the change of R^2 is relatively small, the total number of DGEs changed during aging is much higher than that under paraquat treatment (3578 vs 1203). Thus, the PCA and correlation analysis suggest that aging and paraquat exhibit different impacts on oenocyte translatome, and aged flies showed slightly reduced sensitivity to oxidative stress.

In addition, cluster analysis using hierarchy clustering from R revealed 11 distinct clusters (Figure 2E). Cluster 1 included genes that were up-regulated in aged oenocytes compared to young ones. Gene ontology analysis showed that cluster 1 was enriched with genes in endocytosis, hippo, JAK-STAT, Fanconi anemia pathway, phosphatidylinositol signaling, DNA replication and ubiquitin mediated proteolysis (Figure 2F). Cluster 6 was represented by genes that were down-regulated by aging. Gene ontology analysis revealed an enrichment in proteasome, oxidative phosphorylation, metabolic pathways and fatty acid metabolism (Figure 2G). Cluster 7 contained genes that were repressed by both aging and paraquat treatment, which were enriched in cytoskeleton organization, cellular protein modification and cell cycle (Figure 2H). There were some clusters that contained fewer genes but show interesting patterns. For example, genes in cluster 2 were up-regulated in aging, but down-regulated by paraquat treatment in aged oenocytes. Gene ontology showed an enrichment in endocytosis pathway for

cluster 2. Additionally, genes in cluster 11 were not affected by aging, but up-regulated in aged paraquat-treated oenocytes. This cluster was enriched with Dorso-ventral axis formation.

Finally, we explored oenocyte gene ontology (GO) network using Cytoscape plug-in: ClueGO. Several GO terms are significantly enriched under aging (Figure 3A), such as organelle ribosome, proteasome, mitochondrial respiratory chain, plasma membrane component, rRNA processing and Wnt protein secretion. In contrast, paraquat treatment produced a different set of GO terms (Figure 3B). Under paraquat treatment, fatty acid elongation, fatty acid metabolism, antibacterial humoral response, defense response to gram-positive bacterium, eggshell formation and neuroactive ligand-receptor interaction are enriched. Taken together, these data suggest that aging, a chronic process, induces different cellular responses compared to acute oxidative stress.

Common translational regulation shared between aging and paraquat treatment

Oxidative stress is often associated during tissue aging; however, it is unclear how oxidative stress contributes to aging. Gene ontology analysis for all DEGs under aging (Figure 3A) and paraquat (Figure 3B) are plotted. To dissect the common mechanism underlying both oxidative stress and aging, we examined what genes were commonly regulated by aging and paraquat. Besides the common target genes, about 1597 genes (out of 2189) that are down-regulated only by aging (Figure 3C). These genes are enriched in gene ontology terms: oxidoreductase, ribosome structure, peroxisome and fatty acid metabolism. In addition, 242 genes (out of 834) are specifically repressed by paraquat treatment (Figure 3C). They are enriched for bacterial response and response to external biotic stimulus.

About 146 genes that are up-regulated by both paraquat treatment and aging (Figure 3D). Paraquat and aging both induce DNA-dependent ATPase activity, DNA recombination and DNA repair. Besides these common pathways, aging specifically induced genes in ATP binding, drug metabolism (cytochrome P450), carbohydrate derivative binding and immune response, while paraquat treatment specifically induced response in photo transduction.

GSEA analysis revealed age-related decreases in oenocyte mitochondrial and peroxisome function, and increases in DNA repair

To further understand the signaling pathways regulated by aging and oxidative stress, we performed gene set enrichment analysis (GSEA) using a collection of pre-defined gene sets based on KEGG database. One advantage of GSEA analysis is that it does not rely on arbitrary cut-off to identify significant changes in individual gene expression, rather it searches for

differential expression of all genes within a pathway. We found that 5 different gene sets within which genes were up-regulated with age: mismatch repair, DNA replication, base excision repair, nucleotide excision repair, and fanconi anemia pathways (Table 1). Interestingly, similar pathways (DNA replication, mismatch repair, and fanconi anemia pathway) were found as PQ-induced gene sets. Surprisingly, no pathways are significantly repressed after corrected for multiple tests under PQ comparing to water treated flies, possibly because only 7% genome are altered after 10mM PQ treatment. Some pathways show significance ($p<0.05$) before multiple tests correction: proteasome, lysosome oxidative phosphorylation, peroxisome and fatty acid, nitrogen metabolism are repressed under PQ treatment.

Through GSEA, we discovered 5 pathways within which most of genes were significantly down-regulated during aging: oxidative phosphorylation, ribosome, proteasome, peroxisome, glycolysis/gluconeogenesis pathways, and fatty acid metabolism. Interestingly, most of genes involved in peroxisome receptor recycling, membrane assembly and matrix protein import had decreased expression under aging (Figure 4A). For example, PEX19/Pex19 (human orthologue/*Drosophila* orthologue) is essential for assembling peroxisomal membrane proteins in many species. Pex19 is repressed by 3 fold during aging (Figure 4A). Pex7 and Pex5, which are responsible for import by bringing newly synthesized proteins into peroxisome, showed 7 fold and 3 fold repression under aging (Figure 4A). Interestingly, most of the peroxin (*PEX*) genes showed down-regulation under PQ stress, though to a less extend comparing to aging (Figure 4B). This suggests that oxidative stress might predispose cells to repress peroxisome expression, while aging augmented this effect. In addition, almost all mitochondrial ribosomal subunits (mRpS and mRpL proteins) decreased their expression in both paraquat-treated and aged oenocytes (Figure 4C).

Aged oenocytes show reduced sensitive to paraquat treatment

One of features of aging is a gradual decrease of resistance to stresses, such as oxidative stress as well as heat-shock [37]. The glutathione transferases are important in detoxification process after genotoxic stresses [38]. We found that out of 21 GSTs genes, 5 of them (*sepia*, *GstD2*, *GstD9*, *GstD1* and *GstE11*) are differentially regulated to PQ in young flies but are unchanged in aged. *GstD1* show highest induction (1.5x) upon PQ feeding in young flies, but the level remains unchanged in aged flies (Figure 5A). Furthermore, 4 of GSTs genes were slightly induced in young flies but suppressed in old flies upon PQ stress (see supplementary). Our data

suggests that young flies were able to regulate expression of stress-response genes effectively, whereas in aged flies, this regulation is dampened.

There are 1002 protein-coding genes differentially regulated (2-fold change) by PQ at young age. The number reduced to 385 genes in PQ treated aged flies. 214 genes are up-regulated to PQ stress in young flies, whereas 201 genes are up-regulated in aged (Figure 5B). There is significantly more down-regulated to PQ in young flies (816) than in old flies (184) in figure 5C. Not only had the number of genes in response to oxidative stress reduced during aging, the members of these genes also changed. We selected genes that are 2-fold-change under young-PQ and old-PQ conditions, and overlap them. Only 3 genes were commonly up-regulated between young PQ and old PQ. This indicates there was differential translational regulation to PQ at different ages. In young flies, feeding paraquat will induce expression of genes in mismatch repair, DNA replication, nucleotide excision repair and phototransduction (Figure 5B). However, in old flies, genes in these sets were not up-regulated. Instead, genes found in extracellular matrix and plasma membrane are up-regulated. Gene ontology analysis reveals that at young age, genes involved in metabolic process, response to bacterium, cell cycle response, fatty acid elongation decrease of their expression to paraquat. No significant GO-Biological Process sets are significantly enriched in aged-paraquat (supplementary). It suggests that some genes are actively repressed in young flies upon oxidative stress. Once flies are aged, loss of transcriptional regulation will up-regulate these genes and may be detrimental to the cell. These data indicate dampened and different stress response in aged flies.

Identification of oenocyte-unique genes

To identify genes that are enriched in adult oenocytes, we used Fragments Per Kilobase Million (FPKM) reads from young oenocytes and compared them with *Drosophila* transcriptome database, *Flyatlas 1* [39] and *Flyatlas 2* [40]. We considered genes with no expression in other tissues are the oenocyte-unique genes and genes with more than 5-fold change comparing to whole body expression as oenocyte-enriched genes. We found 17 gene are uniquely expressed in oenocyte (**Table 2**) and 528 oenocyte-enriched genes (Additional file 1, S1). Many of oenocyte-enriched genes are cuticular proteins or regulate structural constituent of chitin-based cuticle. From these oenocyte unique proteins, we identifed *TweedleZ (TwdlZ)* and *TweedleN (TwdlN)*. They are part of Tweedle family that have molecular function in structural constituent of chitin based larval cuticle, regulate body morphogenesis and protenaceous extracellular matrix

formation. *Notum* encodes an enzyme that cleaves Glycophosphatidylinositol (GPI) anchors. It's a secreted antagonist to finely balance Wnt signaling. Even though *Notum* has been extensively studied *Drosophila* wing imaginal discs, its role in adult oenocyte is largely unknown. It's possible that oenocyte regulates neighboring tissue homeostasis by secreting Notum in adult *Drosophila*.

Oenocytes and fat body express different sets of liver-like genes

To further understand whether adult oenocyte is functionally similar to mammalian liver, we searched for human orthologues of oenocyte-enriched genes. Using *Drosophila* RNAi Screening Center (DRSC) Integrative Ortholog Prediction Tool (DIOPT), we identified 1088 human orthologues for 529 oenocyte-enriched genes. There are in total 421 genes enriched in human liver as indicated by The Tissue Atlas, a consortium of expression and localization of human proteins in different tissues and organs. Of 1088 human orthologues, 57 of them are enriched in liver according to The Tissue Atlas (Figure 7A). Although only 13.5% of human orthologues of oenocyte-specific genes were found enriched in liver, the similarity between fly oenocytes share higher similarity to human liver other human tissues. For example, 6.5% in brain; 5.92% in cerebral cortex; 6.75% in skin; 6.15% in fallopian tube; 3.67% in placenta; 2.33% in salivary gland; 7.04% in pancreas and 6.02% in adipose (Figure 7B).

Fat body in *Drosophila* was long established as a liver model [41]. Since oenocytes also exhibit hepatocyte-like functions (e.g., steatosis), it remains to be established whether fat body and oenocytes each resemble different aspects of liver-functions. First, we found that there was very little overlap of enriched genes between fat body and oenocytes (Figure 7C). Gene ontology analysis revealed that fat body mainly contains genes in regulating biosynthesis of antibiotics and amino acids, fatty acid degradation and lysosome (Figure 7D). In contrast, oenocytes are enriched with genes regulating proteasome, biosynthesis of very long-chain fatty acid, wax biosynthesis, ketone body metabolism and xenobiotics by cytochrome P450 (Figure 7D and supplementary S14). Oenocyte's function in very long-chain fatty acid and wax biosynthesis were previously reported [17,42]. These results suggest that adult fat body and oenocytes regulate distinct functions.

Compared to oenocytes, about 1827 human orthologues for 689 genes that are enriched in fly fat body. Of 1827 human orthologues, 141 of them are enriched in human liver (Figure 7E). Interestingly, we found about 16 oenocyte-specific liver orthologues genes that are involved in

ethanol metabolism, ketogenesis, and glucose metabolism (Figure 7F). Fly *CG6432* has multiple human liver orthologues, such as acyl-CoA synthetase medium chain family member 3 (ACSM3), 2B (ACSM2B), 5 (ACSM5) and 2A (ACSM2A). ACSM3 have acyl-CoA ligase activity to modify fatty acids for further processing. The process is the vital first step of fatty acid metabolism [43]. Oenocyte-specific liver orthologues also include two lectin-like receptors (CLEC1B and CLEC4M) and fibroblast growth factor 21 (FGF21), a key hormonal factor that regulates glucose uptake in adipocytes. Taken together, oenocytes not only regulate xenobiotics and steroid hormone biosynthesis, but also function as a metabolic center for ethanol, glucose and fatty acid, like human liver.

From fat body and oenocyte liver orthologues, there were 41 human orthologues shared between two tissues (Figure 7G). Fat body-specific liver orthologues are enriched in complement and coagulation cascades, steroid hormone biosynthesis, drug metabolism, retinol metabolism and glycan biosynthesis/metabolism (Figure 7H). These functions are different from oenocytes. For example, *FGF21/bnl* (human orthologue/*Drosophila*) has no expression in other tissue except in oenocyte. In addition, ketogenesis and pyruvate kinase, which represent hall mark of hepatocyte cells, are not enriched in fat body. We also perform KEGG functional analysis on genes shared between fat body and oenocyte-specific liver orthologues (41 genes). The shared gene list is enriched in Retinol metabolism, metabolism of xenobiotics, linoleic acid metabolism and bile secretion (Figure 7I). Because retinol metabolism and xenobiotics are two major liver functions, our analysis suggests that fat body and oenocytes may share part of the liver function in *Drosophila*.

Conservation of age-related transcriptional changes between oenocytes and liver

To determine whether oenocyte aging shares similar mechanisms as mammalian liver aging, we obtained liver transcriptomic profile from a previous mouse aging study [44]. About 1191 genes differentially expressed in aging liver were first converted to their fly orthologues using DIOPT. We identified 191 genes that are differentially regulated by aging in both mouse liver and oenocyte. Gene ontology analysis identified several common cellular function altered by aging (Figure 7A). Our oenocyte aging data corresponds to what has been observed in aged liver, lipid metabolism, oxidation-reduction process, fatty acid metabolism are also significantly downregulated with aging [44]. In addition, pathways such as insulin signaling and xenobiotics metabolism are also altered during aging. This result agrees with what's observed in aged human

liver, where insulin sensitivity is altered in aging [45]. We also identified CYP3A, a key enzyme for drug metabolism, as an aging-regulated gene shared between liver and oenocytes. Its fly orthologue (Cyp6a8) is down-regulated in aged oenocytes, which is consistent with previous study showing age-dependent reduction of CYP3A-dependent metabolism [46].

In addition, we also identified many oenocytes-specific changes during aging. Using published tissue aging data, we compared age-related gene expression from multiple *Drosophila* tissues, including heart, oenocytes, midgut and fat body (Figure 7B). These tissue-specific DEs were then categorized using PANTHER and DAVID pathway analyses revealed that tissue-specific transcriptional changes during aging. For example, in oenocytes, the expression of genes in structural constituent of ribosome, insulin receptor cascade, peroxisome and mitochondrial translation are significantly altered. Whereas aging fat body showed changes in RNA metabolism, drug metabolism, metabolic pathways and membrane trafficking. Aging mainly affected transporter activity, DNA replication and glycan degradation in midgut. Aging heart showed altered lysosome, actin cytoskeleton, phosphatidylinositol, and phagosome.

Discussion

1. Shared transcription alterations between oenocyte and liver aging

Oenocytes have been recently proposed as hepatocyte-like cells in *Drosophila* [2], because of its steatosis feature under starvation stress. Our translatomic analysis identified many oenocyte-enriched genes that are orthologous to liver specific proteins, highlighting the molecular and functional similarities between the two organs. First, oenocyte is enriched with xenobiotic enzymes for detoxification (Figure 7D). For example, Mgstl/MGST1 (*Drosophila* orthologue/human orthologue) is highly enriched in oenocyte. Its human orthologue is enriched in adipocyte fat and liver. It belongs to the MAPEG (Membrane Associated Proteins in Eicosanoid and Glutathione metabolism) family, in which most proteins are involved in cellular defense against toxic compounds and oxidative stress. In addition, oenocyte is enriched with peroxisomal genes (supplementary data), like liver which also contains abundant peroxisome that is important for fat metabolism, detoxification and bile synthesis. For example, *PEX19*, which regulates peroxisome membrane assembly, has 949 FPKM value comparing to RNA-seq FPKM value from other tissues. This suggests that peroxisome is highly abundant in oenocyte because it's unique requirement for this organelle. In addition, we identify genes that are highly enriched

in oenocyte (at least 5 times higher expression in whole body) and some of them share human liver orthologues. For example, formaldehyde dehydrogenase (*Fdh*). *Fdh* is homologous to human alcohol dehydrogenase 1B (ADH1B), which has biased expression in liver and fat. ADH1B metabolizes substrates such as ethanol, retinol etc. The enzyme exhibits high activity for ethanol oxidation and is important in ethanol catabolism. Because liver contains higher amount of alcohol metabolizing enzymes, liver plays the major role in alcohol metabolism [47–49].

Many of the liver orthologues in oenocyte decrease their expression in aging, correlate to decreased detoxification, alcohol metabolism in liver aging. For example, *CG6432* which is orthologous to human ACSM3, has decreased expression under paraquat and aging. Down regulation of ACSM3 will lead to hepatocellular carcinoma (HCC) by promoting metastasis, suggesting its importance in liver function [50]. Thus, our data suggests oenocyte is like liver by functioning as a major site for fat metabolism, detoxification, ethanol catabolism and they share similar functional decline as liver aging.

2. Impaired mitochondrial function in aging oenocytes

Most of the age-related genes show a gradual expression change from young to old ages after 30-day of age[51]. Flies have a median age at 30-50 days [37]. Thus, we performed Ribo-tag analysis on 4-week-old flies to capture early onset of transcriptional changes that may reflect the initiation of aging program[51]. Our Ribo-tag analysis revealed a decreased expression of mitochondrial ribosome subunits under aging and paraquat treatment. It is well established that aging will compromise mitochondrial function, deregulated nutrient sensing, altered metabolic response and compromised immunity [4].

Mitochondrial ribosomes (mitoribosomes) reside in the matrix of the mitochondria and associate with the inner membrane to assist co-translational insertion of hydrophobic polypeptides. Microribosomes are essential for synthesis of proteins for oxidative phosphorylation. Mutations affecting the rRNA and protein components produce many human mitochondrial diseases, such as leigh's syndrome, encephalomyopathy, sensorineural hearing loss and hypertrophic cardiomyopathy [52]. The RAS/cAMP pathway is the signaling pathway that directly regulate mitochondrial biogenesis. CAMP-dependent, catalytic subunit 3 (Pka-C3), subunit 1 (Pka-C1) both are down regulated under aging condition, but not significantly decreased in paraquat. It's possible that reduced level or activity of Pka-C3 and C1 down-regulate mitochondrial biogenesis genes. In addition, decreased respiratory chain function will alter one carbon metabolism and

lead to serine accumulation. Bao et al. reduced the amount of DNA in the mitochondria in human cells, and it caused the cell to elevate serine biosynthesis [53]. Serine was found to be increased in a mitochondrial Parkinson's disease model in *Drosophila* [54]. Defects in one carbon metabolism could further impact metabolically active cells, which are deprived of essential purine-containing cofactors, such as NAD+ [53]. Interestingly, our aging data also showed that thiamine, carbon, citrate cycle and serine metabolisms are altered during aging. These metabolism pathways rely heavily on mitochondrial protein functions. Alteration of mitochondrial biogenesis lead to higher ROS production, decreased respiratory chain and altered one carbon metabolism, all of which can contribute to the aging process.

3. Impaired peroxisome function in aging oenocytes

Peroxisomes are important subcellular organelles which catalyze many metabolic functions: 1) fatty acid beta-oxidation, especially on very-long-chain fatty acids (VLCFA); 2) lipid biosynthesis; 3) in the liver, peroxisomes are also involved in bile acids synthesis; 4) synthesis of plasmalogens, a family of phospholipids which are important in membrane components [55]. Peroxisome is also important for ROS generation and scavenging. Peroxisomes grow by post-translational import of membrane proteins from the cytosol and then multiply by division of pre-existing organelles [56]. They can be also assembled from endoplasmic reticulum (ER). ER-derived peroxisomal vesicles that carrying different membrane proteins fuse to assemble peroxisomal translocon, which is important for import of protein to peroxisome [57]. Our data revealed that aging and oxidative stress decreased the expression of most of peroxisome biogenesis genes, which is consistent with a previous proteomic study showing that peroxisome protein expression and import decrease in aged *C. elegans* [58]. In *Drosophila*, there are 14 peroxin (PEX) genes, the major peroxisomal biogenesis factors. The expression of 13 peroxin genes decreased under aging, including evolutionarily conserved peroxin genes: *pex5*, *pex7* and *pex19*. *Pex5 and 7* are responsible for peroxisomal protein matrix import. *Pex19* plays important role in peroxisomal membrane assembly. The number of peroxisome is carefully controlled by the cell through biogenesis, degradation (pexophagy), or inheritance (cell division and budding). Interestingly, *CG13827*, encodes a human ortholog Pex11gamma, also shows decreased expression under aging and PQ treatment. Pex11 family contains conserved membrane proteins that have been proposed to control peroxisome proliferation and peroxisomal fission or division, the processes that are followed by dynamin-

like proteins (DLPs/DRPs) to complete fission. Pex11gamma is particularly prominent in the liver. Even though knock out (KO) of Pex11gamma in mice has no noticeable phenotype, KO of Pex11beta results in neonatal lethality and Zellweger-like phenotype. Pex11beta also showed decreased level of expression under aging and PQ. However, Pex11 is not decreased in aged *c.elegans* from previous proteomic analysis [58].

It is known that peroxisome enzyme activity and overall function are compromised in aging rat liver (Perichon, Bourre, Kelly, & Roth, 1998). Peroxisome generates ROS as a feature of its normal metabolism. In fact, peroxisome accounts for ~35% hydrogen peroxide production in liver [60]. Paraquat and aging both reduce expression of PEX genes (required for peroxisome biogenesis) indicates that cells are trying to eliminate peroxisomes as ROS generator. However, peroxisome also contains many antioxidant enzymes that prevent cellular ROS level to increase, such as catalase (CAT), superoxide dismutase 1 (SOD1), peroxiredoxin 5 (Prx5) and microsomal glutathione S-transferse-like (Mgstl) [61]. Inhibition of peroxisome leads to higher ROS level in an aging cell, due to lack of active catalase [61]. Generation of excessive peroxisomal ROS will disturb mitochondria redox balance, leading to mitochondrial dysfunction and tissue aging [62].

Our analysis reveals that genes involved in peroxisomal beta-oxidation is compromised under aging and paraquat treatment. Consistently, peroxisomal beta-oxidation decreases in old mouse liver [63]. Hepatocyte nuclear factor 4 (HNF4) is the major regulate for mitochondrial and peroxisomal β-oxidation, fatty acid desaturation. The expression of oenocyte HNF4 significantly decreased under aging and paraquat. *dHNF4* can regulate lipid mobilization, and it regulates various enzymes involved in peroxisomal β-oxidation, such as acyl-Coenzyme A oxidase at 57D distal (Acox57D-d), acyl-coenzyme A oxidase at 57D proximal (Axoc57-p) are acyl-CoA dehydrogenae/oxidase. Their expression is both decreased during aging and they involved in fatty acid beta-oxidation in *Drosophila*. They both share orthologue with acyl-CoA oxidase 1 (ACOX1) in human. ACOX1 is the first enzyme of the fatty acid beta-oxidation pathway in peroxisome. Defects in this gene will result in pseudo neonatal adrenoleukodystrophy, a disease caused by accumulation of long chain fatty acids. In addition, peroxisome is crucial for fatty acid oxidation. Compounds such as long-chain dicarboxylic and very long-chain monocarboxylic fatty acids are only processed by peroxisomal β-oxidation. Using *c.elegans* model, Weir et al. has discovered that maintaining mitochondrial fission or fusion network homeostasis expand life span via metabolic reprogramming, specifically fatty

acid oxidation (FAO) in coordination with peroxisome. In mice brown adipose tissue (BAT), gastrocnemius muscle and liver, transcripts encoding proteins involved in FAO dropped under aging [64]. Peroxisomal proteins are crucial for fatty acid oxidation. Altered FAO will lead to very long- and long-chain acylcarnitines to elevate. Peroxisomes' function is required for mitochondrial homeostasis increased longevity, suggesting interplay between two organelles [65]. In addition to peroxisome's regulatory role in aging as metabolic center, recent studies have shown peroxisome-mediated metabolism is required for immunity [66]. Decreased immune response is one of the hallmarks of aging [4]. A lack of peroxisomes altered the composition of lipid species, such as ceramide, sphingosine, DHA and arachidonic acids, that will signal the formation of the phagosome and other cellular processes [66].

4. Oenocyte-unique genes and comparison with fat body

We compared 411 oenocyte enriched genes with oenocyte enriched 51 genes identified from Gutierrez et al, 2007 and we identify 14 genes are shared between two studies.

We identify 17 genes that are oenocyte-unique (**Table 1**). From these oenocyte unique proteins, we identify *TweedleZ (TwdlZ)* and *TweedleN (TwdlN)*, which regulates structural constituent of chitin-based cuticle, regulate body morphogenesis and protenaceous extracellular matrix formation. Although TwdlZ and TwdlN's function haven't been well studied, studies in *TwdlD* suggests unconventional role in regulating *Drosophila* body shape as cuticular proteins. The gene family are expressed in gene-specific temporal and spatial patterns. Studies also show that Tweedle proteins are incorporated into larval cuticular structures through cross-linking ability. The gene family contains 27 members and is only found in insects. Each of the 27 members contain an N-terminal signal peptide and they are secreted [67]. The paper suggests Tweedle proteins' role in cross-linking in the cuticle. However, high number of gene duplication events suggest that each family member functions similarly, with differences in expression to determine the organization of the cuticle. Interestingly, a related gene in the silkworm *Bombyx mori* named BmGRP2 has a glycine-rich domain [67]. Such domains are proposed to provide flexibility in insect's cuticle. We find TwdlN also contains glycine-rich domain, which might have distinct role in cuticle formation and affect flexibility.

Our analysis revealed different liver-like functions represented by fat body and oenocyte. Fat body expresses genes that are involved in the production of complement and coagulation factor, steroid hormone biosynthesis, drug metabolism, retinol metabolism, glycine, serine and

559 threonine metabolism. In contrast, different liver-like functions are enriched in oenocytes, such
560 as ketogenesis, ethanol metabolism, and biosynthesis of unsaturated fatty acids. It is likely both
561 fat body and oenocytes regulates different liver-like functions. Therefore, it should be cautious
562 when using either tissue to modeling mammalian liver diseases.
563 Together, our data show that aging and oxidative stress repress the expression of genes in
564 peroxisome biogenesis, peroxisome division and peroxisomal beta-oxidation. Aging and
565 oxidative stress also lead to compromised mitochondrial biogenesis and oxidative
566 phosphorylation. These cellular changes may significantly contribute to tissue aging through the
567 regulation of one carbon metabolism, FAO and immune response. Our studies provide insights
568 into mechanisms of aging related metabolic diseases in liver.
569
570 **Methods**
571 **Fly strains, aging and paraquat treatment**
572 Flies are raised in 12:12 h light:dark cycle at 25 ˚C, 40% relative humidity on agar-based
573 diet with 0.8% cornmeal, 10% sugar, and 2.5% yeast (unless otherwise noted). Fly strains used in
574 the present study are: *w*; P{Desat1-GAL4.E800}4M* (Bloomington stock number 65405), *UAS-*
575 *RpL13A-FLAG* homozygous flies (a gift from Pankaj Kapahi), PromE-Gal4, UAS-CD8::GFP(II)
576 (a gift from Alex Gould). For aging studies, female flies were collected within 3 days (20 female
577 flies per vial) and then flies were transferred to fresh food every 2 days. For paraquat treatment,
578 flies are fed on food containing 10 mM of paraquat at the food surface. Flies are fed for 24 hours
579 prior to each assay.
580 **Starvation assay and Oil Red O staining**
581 Flies were kept in empty vial containing PBS-soaked Kimwipe for 36 hours to induce
582 starvation. Flies were dissected in PBS and fixed in 4% paraformaldehyde in PBS for 20
583 minutes. Specimens were then transferred to a new Kimwipe to remove extra dye, then rinsed
584 twice with distilled water. 0.1% Oil Red O (Alfa Aesar, Tewksbury, MA, USA, catalog number:
585 A12989) was prepared by dissolved how much 0.01g of oil Red O in 10ml of isopropanol,
586 prepared fresh and filtered through a 0.2 μm syringe filter. Specimens were incubated in 0.1%
587 Oil Red O for 20 to 30 minutes. Specimens are blotted onto tissue paper and rinsed twice with
588 distilled water. Mount with ProLong Gold antifade with DAPI and scored for large Oil-Red-O-
589 positive droplets (ThermoFisher Scientific, Waltham, MA, USA, catalog number P36931).

Dihydroethidium (DHE) staining

Young and aged flies were fed on normal food or paraquat (10mM) for 24 hours prior to staining with dihydroethidium (Calbiochem, Burlington, MA, USA, Catalog number: 309800-25MG). Production of ROS is visualized with Olympus BX51WI upright epifluorescence microscopy. Detailed protocols are provided in Owusu-ansah, Yavari, & Banerjee, 2013 with minor modification. Flies were dissected in PBS, to obtain carcass cuticle and remove fat body around the oenocyte. One microliter of reconstituted DHE dye was added to 1ml of Schneiders medium (SM). Tissues are incubated for 5 minutes in a dark chamber, on an orbital shaker. 5ul of Hoechst 33342 (ImmunoChemistry Technologies, Bloomington, MN, USA) was added to 1ml of PBS, and incubate the cells for 5 minutes. Tissues were mounted in PBS and 50% glycerol.

Oenocyte Ribo-tag

Female flies carrying PromE-gal4 (Bloomington number 65406) and UAS-RpL13A-FLAG were collected. Three biological replicates (200 females per replicate) were performed for each experimental condition. We used 50ml vials containing 4 ml of solid medium food. 200ul of 10mM of paraquat (dissolved in water) or water only was distributed evenly on food surface, and air dry for 20 minutes. 2-day-old female, mated once, flies were placed in groups of 20 in each vial and maintained at 25 ℃. Young flies (10-day-old) were fed with paraquat or water food for 24 hours prior Ribo-tag procedure. For aging populations, vials were transferred every 2-3 days, until flies are 28-day-old, then fed with paraquat or water prior to Ribo-tag. Ribo-tag experiments were performed in the 10:00-12:00 PM time period, to avoid circadian effects. Ribo-tag protocol was modified from McKnight Lab [68]. Flies were frozen and ground in nitrogen liquid. The fly powder was further homogenized in a Dounce tissue grinder containing 5 mL of homogenization buffer (50mM Tris, pH 7.4, 100mM KCl, 12mM MgCl2, 1mM DTT, 1% NP-40, 400 units/ml RNAsin, 100ug/ml of cycloheximide, 1mg/ml heparin and Protease inhibitors) to generate a 3% weight/volume homogenate. The homogenate was centrifuged at 10,000 rpm for 10 minutes. The supernatant was first pre-cleaned using SureBeads (By Bio Rad, catalog number: 161-4023) and then incubated with 15ul of anti-FLAG antibody (Sigma-Aldrich, St. Louis, MO, Catalog number: F1804) overnight (about 19 hours) at 4 ^{0}C. The antibody/lysate mixture lysate was then incubated with SureBeads for 3 hours at 4 ^{0}C. Ribosome-bound RNA was purified using Qiagen RNeasy micro plus kit.

Transcriptome library construction and high-throughput sequencing (RNA-seq)

RNA-seq libraries were constructed using 300 ng of total RNA and NEBNext Ultra Directional RNA Library Prep Kit for Illumina (NEB #E7420S/L). Poly(A) mRNA (200bp) was obtained and double-stranded cDNA was synthesized according to company manual. Each library was ligated with a NEBNext Adaptor and barcoded with an adaptor-specific index. Libraries were pooled in equal concentrations. The multiplexed libraries were sequenced using Illumina HiSeq 3000 and single-end 50 bp reads format.

RNA-seq data processing and differential expression analysis

Reads are analyzed using FastQC to check for sequencing quality on Galaxy (https://galaxyproject.org). Then reads are mapped to *D. melanogaster* genome (BDGP Release 6 + ISO1 MT/dm6) using Tophat2 v2.1.0 [69]. Transcripts are reconstructed using Cufflinks v2.2.1 [70] with bias correction. Cuffmerge (http://cole-trapnell-lab.github.io/cufflinks/) was used to merge together 12 cufflinks assemblies to produce a GTF file for further analysis with Cuffdiff. Reads were run through Cuffdiff v2.2.1.3 [71] for differential expression analysis, library are normalized using quantile normalization. Differentially expressed protein-coding transcripts are obtained by selecting genes with false discovery rate ≤ 0.05 and fold-change ≥ 2. Genes that did not meet both ≤ 0.05 and fold-change ≥ 2 criteria was indicated as no-change in figures, tables, and text.

Principal component analysis (PCA)

PCA graph was generated using R package DESeq2 (https://bioconductor.org/packages/release/bioc/html/DESeq2.html), plotPCA function. Data was plotted after variance stabilizing transformation. Heatmap and hierarchy clustering analysis was generated using ggplot, heatmap.2 function. Data was log2 transformed and all reads were added by a pseudo-value 1. Scatter plot is plotted using ggplot2 package.

Oenocyte-enriched genes and tissue aging transcriptome comparison

Oenocyte-enriched genes were identified by comparing mean reads in the present study and other transcriptome studies using fly whole body (obtained from public database GEO). The reads (FPKM ≥ 0.01) are normalized with quantile normalization from preprocessCore package (https://www.bioconductor.org/packages/release/bioc/html/preprocessCore.html). Two genotypes of wild-type whole body RNA-seq were obtained (*w1118:* GSM2647344; GSM2647345; GSM2647345; *yw:* GSM694258; GSM694259) (Chen et al., 2014, unpublished; Oliver B, 2017). Oenocyte-enriched genes were defined as genes with 5 times higher FPKM in

oenocytes than that in whole body. Oenocyte-unique genes were identified as having no expression in other tissues based on Flyatlas 1 (http://flyatlas.gla.ac.uk/flyatlas/index.html) and 2 databases (http://flyatlas.gla.ac.uk/FlyAtlas2/index.html). Fat body-enriched genes were obtained from FlyAtlas database, with a fat:fly score higher than 5 [39].

The lists of differentially expressed genes in multiple fly tissue were extracted from previous transcriptome studies on aging fly tissues. (H. Chen, Zheng, & Zheng, 2014; Girardot, Monnier, & Tricoire, 2004; Resnik-Docampo, 2016, unpublished). Venn diagram analysis (http://bioinformatics.psb.ugent.be/webtools/Venn/) was performed to identify overlapping genes between different conditions. Lists of gene symbols, flybase IDs are used as inputs in the analysis shown in figures.

Gene Set Enrichment Analysis (GSEA)

For GSEA analysis, a complete set of 136 KEGG pathways in *Drosophila* were downloaded from KEGG. Text were trimmed and organized using Java script. Quantile normalized FPKM values for each group were used as input for parametric analysis, and organized as suggested by GSEA tutorial site (GSEA, http://software.broadinstitute.org/gsea/doc/GSEAUserGuideFrame.html) [75]. Collapse dataset to gene symbols was set to false. Permutation type was set to gene set; enrichment statistic used as weighted analysis; metric for ranking genes was set to Signal to Noise.

Gene ontology and pathway analysis

Functional annotation analysis of differentially expressed genes was performed using DAVID and PANTHER. Non-coding gene and low expressed genes (FPKM<0.01) were excluded from the analysis. GO term-biological process enrichment analysis were performed using PANTHER 13.0 database online on age/paraquat up or down-regulated genes [76] (PANTHER, http://www.pantherdb.org/). KEGG pathway enrichment analysis was performed on DAVID v6.8 using default parameters [77] (DAVID, https://david.ncifcrf.gov/). Human orthologues of fly genes, or vice versa, were predicated using DRSC Integrative Ortholog Prediction Tool with “exclude low ranked score” option [78], (DIOPT, http://www.flyrnai.org/diopt).

Acknowledgements

We thank Bloomington Drosophila Stock Center, Pankaj Kapahi, Alex Gould, Joel Levine for fly stocks, reagents and protocols. Michael Baker and DNA Facility at ISU for help with RNA-seq analysis. This work was supported by NIH/NIA R00 AG048016 and Glenn/AFAR Scholarships for Research in the Biology of Aging to KH.

Author Contributions Statement

Conceived and designed the experiments: KH HB. Performed the experiments: KH WC HB. Analyzed the data: KH WC HB. Wrote the paper: KC HB. All authors reviewed and approved the manuscript.

Competing Interests

The authors declare that no competing interest exists.

Figure Legends

Figure 1. Characterization of Drosophila oenocytes at adult stage. A) Lipid droplet formation by oil red O staining of starved wild-type adult flies, the number of lipid droplets in adult oenocytes increased significantly upon starvation. B) Dihydroethidium (DHE) dye was used to examine the impacts of aging and oxidative stress on ROS levels of Drosophila oenocytes. Both aging and oxidant paraquat (PQ) treatment significantly increased ROS levels in adult oenocytes at 2 weeks (young) and 4 weeks (middle age). C) Young oenocytes showed much higher induction of ROS under 10 mM of PQ treatment than did oenocytes from middle age. E) The expression of desat1-E was highly enriched in anti-FLAG immunoprecipitated sample (IP) compared to the input (whole body). F) Average mRNA levels pulled down from the two control groups: (1) Immunoprecipitation of oenocyte-specific RpL13A-FLAG expressing females using only magnetic beads without adding FLAG antibody; 2) Immunoprecipitation of control flies without RpL13A-FLAG expression are undetectable. The scale bar is 10μm.

Figure 2: Genomic analysis on aging or paraquat treated flies. A) principal component analysis (PCA) on the fragments per kilobase million (FPKM) reads. The first component accounts for 50% of the variance and the second component accounts for 9% of variance. B-C)

Correlation analysis using FPKM reads from all four groups. The coefficient of determination (R2) between water-old and water-young groups is 0.861; R2 between water-young and paraquat-young is 0.926; R2 between paraquat-old and water-old is 0.948. Aging induced a bigger transcriptional shift compared to paraquat treatment. E) Cluster analysis using hierarchy clustering from R revealed 11 distinct clusters. F-G) Gene Ontology analysis on cluster 1, 6 and 7.

Figure 3: Common translational regulation shared and distinct regulation between aging and paraquat treatment. A-B) Gene ontology analysis for all DEGs under aging and paraquat. C) About 1597 genes (out of 2189) that are down-regulated only by aging. D) 146 genes that are up-regulated by both paraquat treatment and aging.

Figure 4: GSEA enrichment analysis changed peroxisome and mitochondrial ribosome under aging and paraquat. A) Genes involved in peroxisome receptor recycling, membrane assembly and matrix protein import had decreased expression under aging. B) Most of the peroxin (PEX) genes showed down-regulation under PQ stress, though to a less extend comparing to aging. C) Almost all mitochondrial ribosomal subunits (mRpS and mRpL proteins) decreased their expression in both paraquat-treated and aged oenocytes.

Figure 5: Aged oenocytes show reduced sensitive to paraquat treatment. A) GstD1 show highest induction (1.5x) upon PQ feeding in young flies, but the level remains unchanged in aged flies. B) The paraquat induced genes overlap between young and aged flies. C) The paraquat repressed genes overlap between young and aged flies.

Figure 6: Oenocytes and fat body express different sets of liver-like genes. A) Overlapping analysis between oenocyte-human orthologues and liver enriched genes. There are in total 421 genes enriched in human liver as indicated by The Tissue Atlas, a consortium of expression and localization of human proteins in different tissues and organs. Of 1088 human orthologues converted from oenocytes, 57 of them are enriched in liver. B) The percent of similarity between fly oenocytes to human liver is higher than other human tissues. 6.5% in brain; 5.92% in cerebral cortex; 6.75% in skin; 6.15% in fallopian tube; 3.67% in placenta; 2.33% in salivary gland;

7.04% in pancreas and 6.02% in adipose. C) Overlap of enriched genes between fat body and oenocytes. D) Gene ontology analysis revealed that fat body mainly contains genes in regulating biosynthesis of antibiotics and amino acids, fatty acid degradation and lysosome. E) Compared to oenocytes, about 1827 human orthologues for 689 genes that are enriched in fly fat body. Of 1827 human orthologues, 141 of them are enriched in human liver. F) 16 oenocyte-specific liver orthologues genes that are involved in ethanol metabolism, ketogenesis, and glucose metabolism. G) From fat body and oenocyte liver orthologues, there were 41 human orthologues shared between two tissues. H) Fat body-specific liver orthologues are enriched in complement and coagulation cascades, steroid hormone biosynthesis, drug metabolism, retinol metabolism and glycan biosynthesis/metabolism. I) KEGG functional analysis on genes shared between fat body and oenocyte-specific liver orthologues: gene list is enriched in Retinol metabolism, metabolism of xenobiotics, linoleic acid metabolism and bile secretion.

Figure 7: Conservation of age-related transcriptional changes between oenocytes and liver. A) 1191 genes differentially expressed in aging liver were first converted to their fly orthologues using DIOPT. 191 genes are differentially regulated by aging in both mouse liver and oenocyte. Gene ontology analysis identified several common cellular function altered by aging. B) Many oenocytes-specific changes during aging. Using published tissue aging data, age-related gene expression from multiple Drosophila tissues, including heart, oenocytes, midgut and fat body overlap to reveal oenocyte-specific changes.

776 **References**

777

778 1. Makki R, Cinnamon E, Gould AP. The Development and Functions of Oenocytes. Annu Rev
779 Entomol [Internet]. 2014;59:405–25. Available from:
780 http://www.annualreviews.org/doi/10.1146/annurev-ento-011613-162056
781 2. Gutierrez E, Wiggins D, Fielding B, Gould AP. Specialized hepatocyte-like cells regulate
782 Drosophila lipid metabolism. Nature. 2007;445:275–80.
783 3. Martins GF, Ramalho-Ortigão JM, Lobo NF, Severson DW, McDowell MA, Pimenta PFP.
784 Insights into the transcriptome of oenocytes from Aedes aegypti pupae. Mem Inst
785 Oswaldo Cruz [Internet]. Fundação Oswaldo Cruz; 2011 [cited 2017 Dec 28];106:308–
786 15. Available from: http://www.scielo.br/scielo.php?script=sci_arttext&pid=S0074-
787 02762011000300009&lng=en&tlng=en
788 4. López-Otín C, Blasco MA, Partridge L, Serrano M, Kroemer G. The hallmarks of aging. Cell.
789 2013;153.
790 5. Kim IH, Kisseleva T, Brenner DA. Aging and liver disease. Curr Opin Gastroenterol
791 [Internet]. NIH Public Access; 2015 [cited 2018 Jan 24];31:184–91. Available from:
792 http://www.ncbi.nlm.nih.gov/pubmed/25850346
793 6. Schmucker DL. Age-related changes in liver structure and function: Implications for disease ?
794 Exp Gerontol [Internet]. Pergamon; 2005 [cited 2017 Dec 13];40:650–9. Available from:
795 http://www.sciencedirect.com/science/article/pii/S0531556505001191?via%3Dihub
796 7. Bloomer SA, Zhang HJ, Brown KE, Kregel KC. Differential Regulation of Hepatic Heme
797 Oxygenase-1 Protein With Aging and Heat Stress. Journals Gerontol Ser A Biol Sci Med
798 Sci [Internet]. 2009 [cited 2018 Jan 29];64A:419–25. Available from:
799 http://www.ncbi.nlm.nih.gov/pubmed/19196643
800 8. Hong I-H, Lewis K, Iakova P, Jin J, Sullivan E, Jawanmardi N, et al. Age-associated Change
801 of C/EBP Family Proteins Causes Severe Liver Injury and Acceleration of Liver
802 Proliferation after CCl_4 Treatments. J Biol Chem [Internet]. 2014 [cited 2018 Jan
803 29];289:1106–18. Available from: http://www.ncbi.nlm.nih.gov/pubmed/24273171
804 9. Hong I-H, Lewis K, Iakova P, Jin J, Sullivan E, Jawanmardi N, et al. Age-associated Change
805 of C/EBP Family Proteins Causes Severe Liver Injury and Acceleration of Liver
806 Proliferation after CCl_4 Treatments. J Biol Chem. 2014;289:1106–18.

807 10. Jin J, Iakova P, Breaux M, Sullivan E, Jawanmardi N, Chen D, et al. Increased Expression of
808 Enzymes of Triglyceride Synthesis Is Essential for the Development of Hepatic Steatosis.
809 Cell Rep [Internet]. 2013 [cited 2018 Jan 29];3:831–43. Available from:
810 http://www.ncbi.nlm.nih.gov/pubmed/23499441
811 11. Amir M, Czaja MJ. Autophagy in nonalcoholic steatohepatitis. Expert Rev Gastroenterol
812 Hepatol [Internet]. 2011 [cited 2018 Jan 29];5:159–66. Available from:
813 http://www.ncbi.nlm.nih.gov/pubmed/21476911
814 12. Amir M, Czaja MJ. Autophagy in nonalcoholic steatohepatitis. Expert Rev Gastroenterol
815 Hepatol. 2011;5:159–66.
816 13. Sheedfar F, Biase S Di, Koonen D, Vinciguerra M. Liver diseases and aging: Friends or
817 foes? Aging Cell. 2013;12:950–4.
818 14. Franceschi C, Bonafè M, Valensin S, Olivieri F, De Luca M, Ottaviani E, et al. Inflamm-
819 aging. An evolutionary perspective on immunosenescence. Ann N Y Acad Sci.
820 2000;908:244–54.
821 15. Cui H, Kong Y, Zhang H. Oxidative stress, mitochondrial dysfunction, and aging. J Signal
822 Transduct [Internet]. Hindawi; 2012 [cited 2017 Dec 24];2012:646354. Available from:
823 http://www.ncbi.nlm.nih.gov/pubmed/21977319
824 16. Ristow M, Schmeisser S. Extending life span by increasing oxidative stress. Free Radic Biol
825 Med [Internet]. Pergamon; 2011 [cited 2018 Jan 31];51:327–36. Available from:
826 https://www.sciencedirect.com/science/article/pii/S0891584911003121
827 17. Billeter J-C, Atallah J, Krupp JJ, Millar JG, Levine JD. Specialized cells tag sexual and
828 species identity in Drosophila melanogaster. Nature [Internet]. Nature Publishing Group;
829 2009;461:987–91. Available from:
830 http://www.nature.com/doifinder/10.1038/nature08495
831 18. Shirangi TR, Dufour HD, Williams TM, Carroll SB. Rapid Evolution of Sex Pheromone-
832 Producing Enzyme Expression in Drosophila. Eisen MB, editor. PLoS Biol [Internet].
833 Public Library of Science; 2009 [cited 2018 Jan 31];7:e1000168. Available from:
834 http://dx.plos.org/10.1371/journal.pbio.1000168
835 19. Johnson MB, Butterworth FM. Maturation and aging of adult fat body and oenocytes
836 inDrosophila as revealed by light microscopic morphometry. J Morphol [Internet]. Wiley
837 Subscription Services, Inc., A Wiley Company; 1985 [cited 2018 Jan 31];184:51–9.

838 Available from: http://doi.wiley.com/10.1002/jmor.1051840106
839 20. Tower J, Landis G, Gao R, Luan A, Lee J, Sun Y. Variegated expression of Hsp22 transgenic
840 reporters indicates cell-specific patterns of aging in Drosophila oenocytes. J Gerontol A
841 Biol Sci Med Sci [Internet]. Oxford University Press; 2014 [cited 2018 Jan 31];69:253–9.
842 Available from: http://www.ncbi.nlm.nih.gov/pubmed/23723429
843 21. Sanz E, Yang L, Su T, Morris DR, Mcknight GS, Amieux PS, et al. Cell-type-specific
844 isolation of ribosome-associated mRNA from complex tissues. [cited 2017 Dec 28];
845 Available from: http://faculty.washington.edu/dmorris/RiboTag/Sanz.pdf
846 22. Anglas Jules Philippe Louis. Observations sur les métamorphoses internes de la guêpe et de
847 l'abeille Jules Philippe Louis Anglas,... [Internet]. 1869 [cited 2018 Feb 4]. Available
848 from:
849 http://bibliotheque.bordeaux.fr/in/faces/details.xhtml?id=mgroup%3Ap+unimarcbu_9791
850 33&jscheck=1
851 23. Stendell W. Beitr ägе zur Kenntnis der Oenocyten von Ephestia kuehniella Zeller. Zeitschr f
852 Wissensch Zool. 1912;102.
853 24. Wigglesworth VB. Structural lipids in the insect cuticle and the function of the oenocytes.
854 Tissue Cell. 1970;2:155–79.
855 25. Wigglesworth VB. The Physiology of the Cuticle and of Ecdysis in Rhodnius prolixus
856 (Triatomidae, Hemiptera); with special reference to the function of the oenocytes and of
857 the dermal glands. Quart J Micr Sci. 1933;76:269–318.
858 26. Dorn A, Romer F. Structure and function of prothoracic glands and oenocytes in embryos
859 and last larval instars of Oncopeltus fasciatus Dallas (Insecta, Heteroptera). Cell Tissue
860 Res. 1976;171:331–50.
861 27. Locke M. The ultrastructure of the oenocytes in the moltiintermolt cycle of an insect. Tissue
862 Cell. 1969;1:103–54.
863 28. Romer F. Ultrastructural changes of the oenocytes of Gryllus bimaculatus DEG (Saltatoria,
864 Insecta) during the moulting cycle. Cell Tissue Res. 1974;151:27–46.
865 29. Romer F, Bressel HU. Secretion and Metabolism of Ecdysteroids by Oenocyte-Fat Body
866 Complexes (OEFC) in Adult Males of Gryllus bimaculatus DEG (Insecta). Zeitschrift fur
867 Naturforsch - Sect C J Biosci. 1994;49:871–80.
868 30. G. K. Uber den Fettk ¨orper und dieŒnocyten der honigbiene (Apis mellifica. Zool Anz.

1990;337–53.

31. Pantel J. Le Trixion halidayanum Rend. Essai monographique sur les caract ères ext érieurs, la biologie et l'anatomie d'une larve parasite des Tachinaires. Cellule. 1893;15:5–290.

32. R''ossigH. Vonwelchen Organen der Gallwespenlarven geht derReiz zur Bildung der Pflanzengalle aus? Untersuchung derDr ¨usenorgane derGallwespenlarven, zugleich ein Beitrag zur postembryonalen Entwicklung derselben. Zool Jahrb. 1904;19–90.

33. L. S. Recherches morphologiques sur quelques mellif `eres solitaires. Bull Sci Fr Belg. 1906;291–439.

34. R. W. ¨Uber Œnocyten von Torymus nigricornis Boh. mit besonderer Ber¨ucksichtigung derMetamorphose. Zool JahrbAnat. 1907;231–68.

35. Moussian B, Schwarz H, Bartoszewski S, N üsslein-Volhard C. Involvement of chitin in exoskeleton morphogenesis in *Drosophila melanogaster*. J Morphol [Internet]. Wiley Subscription Services, Inc., A Wiley Company; 2005 [cited 2018 Jan 8];264:117–30. Available from: http://doi.wiley.com/10.1002/jmor.10324

36. Qiu J, Hardin PE. Temporal and Spatial Expression of an Adult Cuticle Protein Gene from Drosophila Suggests That Its Protein Product May Impart Some Specialized Cuticle Function. Dev Biol [Internet]. 1995 [cited 2018 Jan 8];167:416–25. Available from: http://www.ncbi.nlm.nih.gov/pubmed/7875368

37. Zou S, Meadows S, Sharp L, Jan LY, Nung Jan Y. Genome-wide study of aging and oxidative stress response in Drosophila melanogaster. 2000 [cited 2017 Dec 31]; Available from: https://pdfs.semanticscholar.org/7156/4cd764174ac39511f06dc3a35faffc26f05c.pdf

38. Sheehan D, Meade G, Foley VM, Dowd CA. Structure, function and evolution of glutathione transferases: implications for classification of non-mammalian members of an ancient enzyme superfamily. Biochem J [Internet]. 2001 [cited 2018 Feb 12];360:1–16. Available from: http://www.ncbi.nlm.nih.gov/pubmed/11695986

39. Chintapalli VR, Wang J, Dow JAT. Using FlyAtlas to identify better Drosophila melanogaster models of human disease. Nat Genet [Internet]. Nature Publishing Group; 2007 [cited 2017 Dec 26];39:715–20. Available from: http://www.nature.com/doifinder/10.1038/ng2049

40. Leader DP, Krause SA, Pandit A, Davies SA, Dow JAT. FlyAtlas 2: a new version of the

900 Drosophila melanogaster expression atlas with RNA-Seq, miRNA-Seq and sex-specific
901 data. Nucleic Acids Res [Internet]. 2017 [cited 2017 Dec 29]; Available from:
902 http://academic.oup.com/nar/article/doi/10.1093/nar/gkx976/4563305/FlyAtlas-2-a-new-
903 version-of-the-Drosophila
904 41. Pandey UB, Nichols CD. Human disease models in Drosophila melanogaster and the role of
905 the fly in therapeutic drug discovery. Pharmacol Rev [Internet]. American Society for
906 Pharmacology and Experimental Therapeutics; 2011 [cited 2018 Feb 13];63:411–36.
907 Available from: http://www.ncbi.nlm.nih.gov/pubmed/21415126
908 42. Agholme L, Agnello M, Agostinis P, Aguirre-ghiso JA, Ahn HJ, Ait-mohamed O, et al. of
909 assays for monitoring autophagy © 2012 Landes Bioscience . Do not distribute . © 2012
910 Landes Bioscience . Do not distribute . 2012;445–544.
911 43. van der Sluis R, Erasmus E. Xenobiotic/medium chain fatty acid: CoA ligase – a critical
912 review on its role in fatty acid metabolism and the detoxification of benzoic acid and
913 aspirin. Expert Opin Drug Metab Toxicol [Internet]. 2016 [cited 2018 Feb 13];12:1169–
914 79. Available from: http://www.ncbi.nlm.nih.gov/pubmed/27351777
915 44. White RR, Milholland B, MacRae SL, Lin M, Zheng D, Vijg J. Comprehensive
916 transcriptional landscape of aging mouse liver. BMC Genomics [Internet]. BMC
917 Genomics; 2015;16:899. Available from: http://www.biomedcentral.com/1471-
918 2164/16/899
919 45. Schmucker DL, Sanchez H. Liver regeneration and aging: a current perspective. Curr
920 Gerontol Geriatr Res [Internet]. Hindawi; 2011 [cited 2017 Dec 13];2011:526379.
921 Available from: http://www.ncbi.nlm.nih.gov/pubmed/21912543
922 46. Cotreau MM, von Moltke LL, Greenblatt DJ. The Influence of Age and Sex on the Clearance
923 of Cytochrome P450 3A Substrates. Clin Pharmacokinet [Internet]. Springer International
924 Publishing; 2005 [cited 2017 Dec 14];44:33–60. Available from:
925 http://link.springer.com/10.2165/00003088-200544010-00002
926 47. DiPadova C, Worner TM, Julkunen RJ, Lieber CS. Effects of fasting and chronic alcohol
927 consumption on the first-pass metabolism of ethanol. Gastroenterology [Internet]. 1987
928 [cited 2018 Jan 7];92:1169–73. Available from:
929 http://www.ncbi.nlm.nih.gov/pubmed/3557012
930 48. Levitt MD, Furne J, DeMaster E. First-pass metabolism of ethanol is negligible in rat gastric

mucosa. Alcohol Clin Exp Res [Internet]. 1997 [cited 2018 Jan 7];21:293–7. Available from: http://www.ncbi.nlm.nih.gov/pubmed/9113266

49. Lee S-L, Chau G-Y, Yao C-T, Wu C-W, Yin S-J. Functional Assessment of Human Alcohol Dehydrogenase Family in Ethanol Metabolism: Significance of First-Pass Metabolism. Alcohol Clin Exp Res [Internet]. 2006 [cited 2018 Jan 7];30:1132–42. Available from: http://www.ncbi.nlm.nih.gov/pubmed/16792560

50. Ruan H-Y, Yang C, Tao X-M, He J, Wang T, Wang H, et al. Downregulation of ACSM3 promotes metastasis and predicts poor prognosis in hepatocellular carcinoma. Am J Cancer Res [Internet]. 2017 [cited 2018 Jan 9];7:543–53. Available from: http://www.ncbi.nlm.nih.gov/pubmed/28401010

51. Zhan M, Yamaza H, Sun Y, Sinclair J, Li H, Zou S. Temporal and spatial transcriptional profiles of aging in Drosophila melanogaster. Genome Res [Internet]. Cold Spring Harbor Laboratory Press; 2007 [cited 2018 Jan 12];17:1236–43. Available from: http://www.ncbi.nlm.nih.gov/pubmed/17623811

52. Rötig A. Human diseases with impaired mitochondrial protein synthesis. Biochim Biophys Acta - Bioenerg [Internet]. Elsevier; 2011 [cited 2018 Jan 5];1807:1198–205. Available from: http://www.sciencedirect.com/science/article/pii/S0005272811001526?via%3Dihub

53. Bao XR, Ong S-E, Goldberger O, Peng J, Sharma R, Thompson DA, et al. Mitochondrial dysfunction remodels one-carbon metabolism in human cells. Elife [Internet]. eLife Sciences Publications Limited; 2016 [cited 2018 Jan 3];5:e10575. Available from: https://elifesciences.org/articles/10575

54. Tufi R, Gandhi S, de Castro IP, Lehmann S, Angelova PR, Dinsdale D, et al. Enhancing nucleotide metabolism protects against mitochondrial dysfunction and neurodegeneration in a PINK1 model of Parkinson's disease. Nat Cell Biol [Internet]. Nature Publishing Group; 2014 [cited 2018 Jan 6];16:157–66. Available from: http://www.nature.com/articles/ncb2901

55. Cooper GM. Peroxisomes. Sinauer Associates; 2000 [cited 2018 Jan 6]; Available from: https://www.ncbi.nlm.nih.gov/books/NBK9930/

56. Bonekamp NA, Völkl A, Fahimi HD, Schrader M. Reactive oxygen species and peroxisomes: Struggling for balance. BioFactors [Internet]. Wiley Subscription Services,

962 Inc., A Wiley Company; 2009 [cited 2018 Feb 22];35:346–55. Available from:
963 http://doi.wiley.com/10.1002/biof.48
964 57. Tabak HF, Braakman I, Zand A van der. Peroxisome Formation and Maintenance Are
965 Dependent on the Endoplasmic Reticulum. Annu Rev Biochem [Internet]. 2013 [cited
966 2018 Jan 6];82:723–44. Available from: http://www.ncbi.nlm.nih.gov/pubmed/23414306
967 58. Narayan V, Ly T, Pourkarimi E, Murillo AB, Gartner A, Lamond AI, et al. Deep Proteome
968 Analysis Identifies Age-Related Processes in C. elegans. Cell Syst [Internet]. The
969 Authors; 2016;3:144–59. Available from: http://dx.doi.org/10.1016/j.cels.2016.06.011
970 59. Perichon R, Bourre JM, Kelly JF, Roth GS. The role of peroxisomes in aging. Cell Mol Life
971 Sci [Internet]. Birkhäuser Verlag; 1998 [cited 2018 Jan 4];54:641–52. Available from:
972 http://link.springer.com/10.1007/s000180050192
973 60. Boveris A, Oshino N, Chance B. The cellular production of hydrogen peroxide. Biochem J
974 [Internet]. Portland Press Limited; 1972 [cited 2018 Jan 4];128:617–30. Available from:
975 http://www.ncbi.nlm.nih.gov/pubmed/4404507
976 61. Fransen M, Nordgren M, Wang B, Apanasets O. Role of peroxisomes in ROS/RNS-
977 metabolism: Implications for human disease. Biochim Biophys Acta - Mol Basis Dis
978 [Internet]. Elsevier; 2012 [cited 2018 Jan 4];1822:1363–73. Available from:
979 https://www.sciencedirect.com/science/article/pii/S0925443911002791
980 62. Ivashchenko O, Van Veldhoven PP, Brees C, Ho Y-S, Terlecky SR, Fransen M.
981 Intraperoxisomal redox balance in mammalian cells: oxidative stress and interorganellar
982 cross-talk. Mol Biol Cell [Internet]. American Society for Cell Biology; 2011 [cited 2018
983 Jan 4];22:1440–51. Available from: http://www.ncbi.nlm.nih.gov/pubmed/21372177
984 63. Périchon R, Bourre JM. Peroxisomal β-oxidation activity and catalase activity during
985 development and aging in mouse liver. Biochimie [Internet]. Elsevier; 1995 [cited 2018
986 Jan 4];77:288–93. Available from:
987 http://www.sciencedirect.com/science/article/pii/0300908496881387?via%3Dihub
988 64. Houtkooper RH, Argmann C, Houten SM, Cantó C, Jeninga EH, Andreux PA, et al. The
989 metabolic footprint of aging in mice. Sci Rep [Internet]. Nature Publishing Group; 2011
990 [cited 2018 Jan 4];1:134. Available from: http://www.nature.com/articles/srep00134
991 65. Weir HJ, Yao P, Huynh FK, Escoubas CC, Goncalves RL, Burkewitz K, et al. Dietary
992 Restriction and AMPK Increase Lifespan via Mitochondrial Network and Peroxisome

993 Remodeling. Cell Metab. 2017;26:884–896.e5.
994 66. Di Cara F, Sheshachalam A, Braverman NE, Rachubinski RA, Simmonds AJ. Peroxisome-
995 Mediated Metabolism Is Required for Immune Response to Microbial Infection.
996 Immunity [Internet]. Elsevier Inc.; 2017;47:93–106.e7. Available from:
997 http://dx.doi.org/10.1016/j.immuni.2017.06.016
998 67. Guan X, Middlebrooks BW, Alexander S, Wasserman SA. Mutation of TweedleD, a
999 Member of an Unconventional Cuticle Protein Family, Alters Body Shape in Drosophila.
1000 Proc Natl Acad Sci U S A [Internet]. 2006 [cited 2017 Dec 30];103:16794–9. Available
1001 from: http://www.jstor.org/stable/30051749
1002 68. Sanz E, Yang L, Su T, Morris DR, McKnight GS, Amieux PS. Cell-type-specific isolation of
1003 ribosome-associated mRNA from complex tissues. Proc Natl Acad Sci U S A [Internet].
1004 2009;106:13939–44. Available from: http://www.pnas.org/content/106/33/13939.full
1005 69. Kim D, Pertea G, Trapnell C, Pimentel H, Kelley R, Salzberg SL. TopHat2: accurate
1006 alignment of transcriptomes in the presence of insertions, deletions and gene fusions.
1007 Genome Biol [Internet]. BioMed Central; 2013 [cited 2018 Feb 14];14:R36. Available
1008 from: http://genomebiology.biomedcentral.com/articles/10.1186/gb-2013-14-4-r36
1009 70. Kim D, Pertea G, Trapnell C, Pimentel H, Kelley R, Salzberg SL. TopHat2: accurate
1010 alignment of transcriptomes in the presence of insertions, deletions and gene fusions.
1011 Genome Biol. BioMed Central; 2013;14:R36.
1012 71. Trapnell C, Hendrickson DG, Sauvageau M, Goff L, Rinn JL, Pachter L. Differential
1013 analysis of gene regulation at transcript resolution with RNA-seq. Nat Biotechnol
1014 [Internet]. NIH Public Access; 2013 [cited 2018 Feb 14];31:46–53. Available from:
1015 http://www.ncbi.nlm.nih.gov/pubmed/23222703
1016 72. Chen Z-X, Sturgill D, Qu J, Jiang H, Park S, Boley N, et al. Comparative validation of the D.
1017 melanogaster modENCODE transcriptome annotation. Genome Res [Internet]. 2014
1018 [cited 2017 Dec 26];24:1209–23. Available from:
1019 http://www.ncbi.nlm.nih.gov/pubmed/24985915
1020 73. Girardot F, Monnier V, Tricoire H. Genome wide analysis of common and specific stress
1021 responses in adult drosophila melanogaster. BMC Genomics [Internet]. BioMed Central;
1022 2004 [cited 2017 Dec 11];5:74. Available from:
1023 http://bmcgenomics.biomedcentral.com/articles/10.1186/1471-2164-5-74

74. Chen H, Zheng X, Zheng Y. Age-associated loss of lamin-B leads to systemic inflammation and gut hyperplasia. Cell [Internet]. Elsevier; 2014 [cited 2017 Dec 10];159:829–43. Available from: http://www.ncbi.nlm.nih.gov/pubmed/25417159

75. Subramanian A, Tamayo P, Mootha VK, Mukherjee S, Ebert BL, Gillette MA, et al. Gene set enrichment analysis: A knowledge-based approach for interpreting genome-wide expression profiles. Proc Natl Acad Sci [Internet]. 2005;102:15545–50. Available from: http://www.pnas.org/cgi/doi/10.1073/pnas.0506580102

76. Thomas PD, Kejariwal A, Guo N, Mi H, Campbell MJ, Muruganujan A, et al. Applications for protein sequence-function evolution data: mRNA/protein expression analysis and coding SNP scoring tools. Nucleic Acids Res [Internet]. Oxford University Press; 2006 [cited 2017 Dec 26];34:W645–50. Available from: https://academic.oup.com/nar/article-lookup/doi/10.1093/nar/gkl229

77. Huang DW, Sherman BT, Lempicki RA. Systematic and integrative analysis of large gene lists using DAVID bioinformatics resources. Nat Protoc [Internet]. Nature Publishing Group; 2008 [cited 2017 Dec 26];4:44–57. Available from: http://www.nature.com/doifinder/10.1038/nprot.2008.211

78. Hu Y, Flockhart I, Vinayagam A, Bergwitz C, Berger B, Perrimon N, et al. An integrative approach to ortholog prediction for disease-focused and other functional studies. BMC Bioinformatics [Internet]. BioMed Central; 2011 [cited 2017 Nov 22];12:357. Available from: http://www.ncbi.nlm.nih.gov/pubmed/21880147

Figure 1

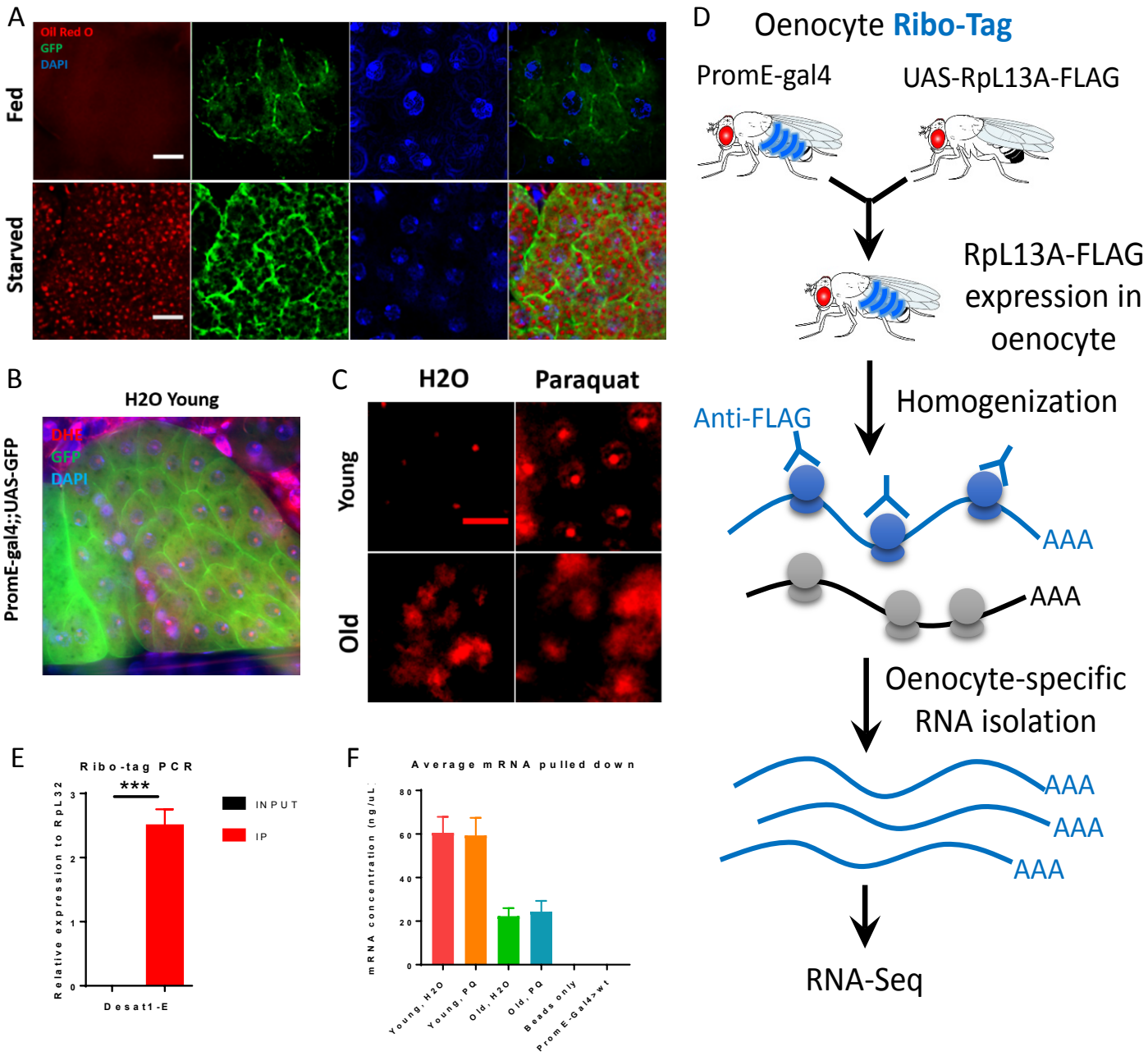

Figure 2

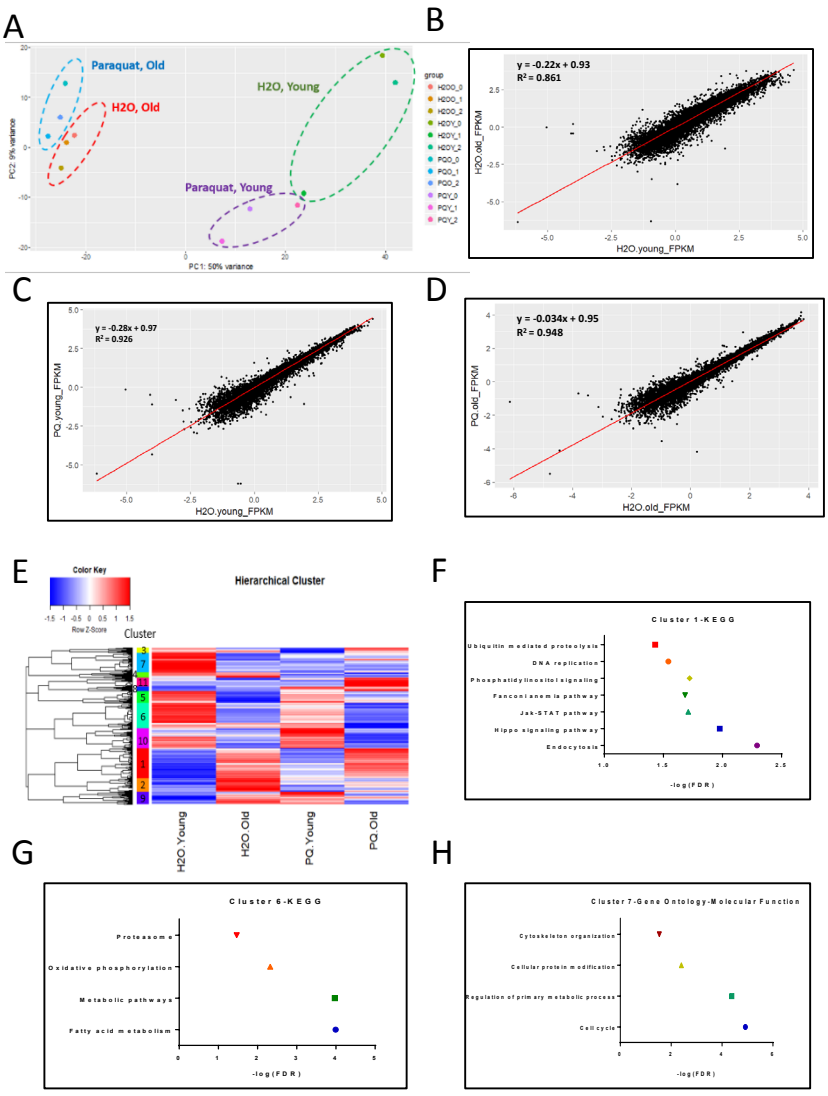

Figure 3

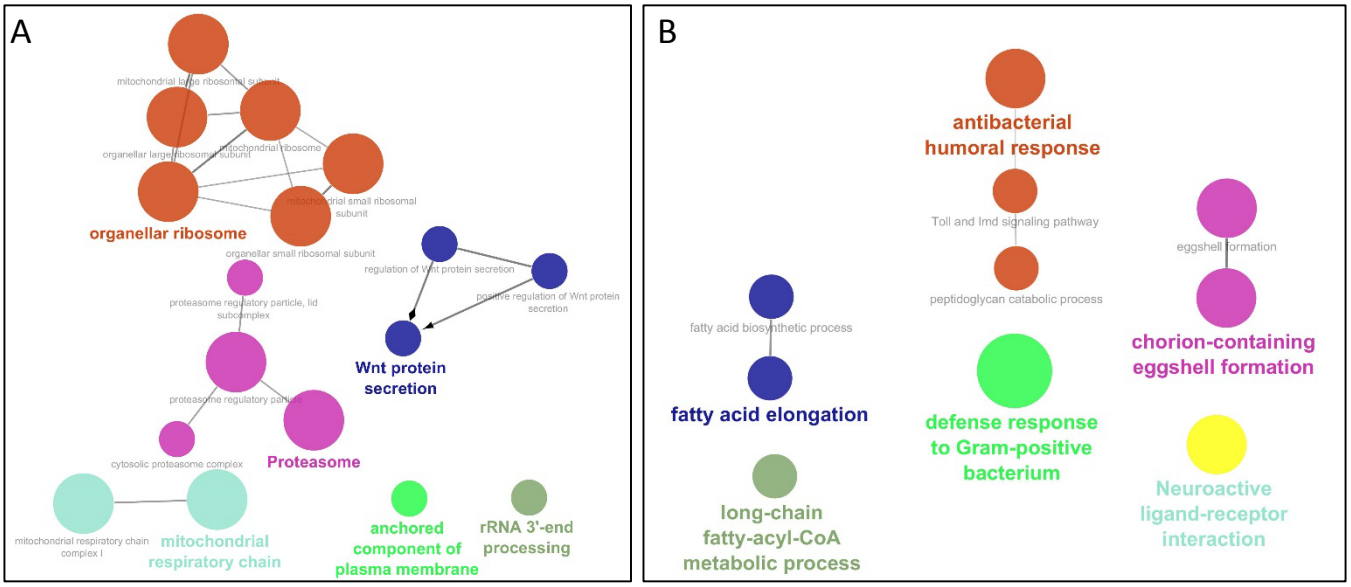

Aging

Paraquat

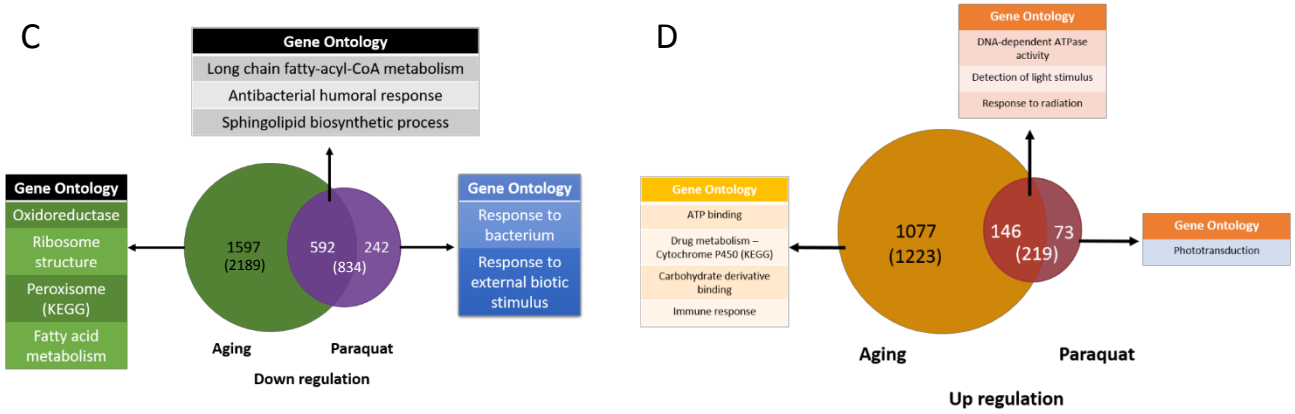

Figure 4

A

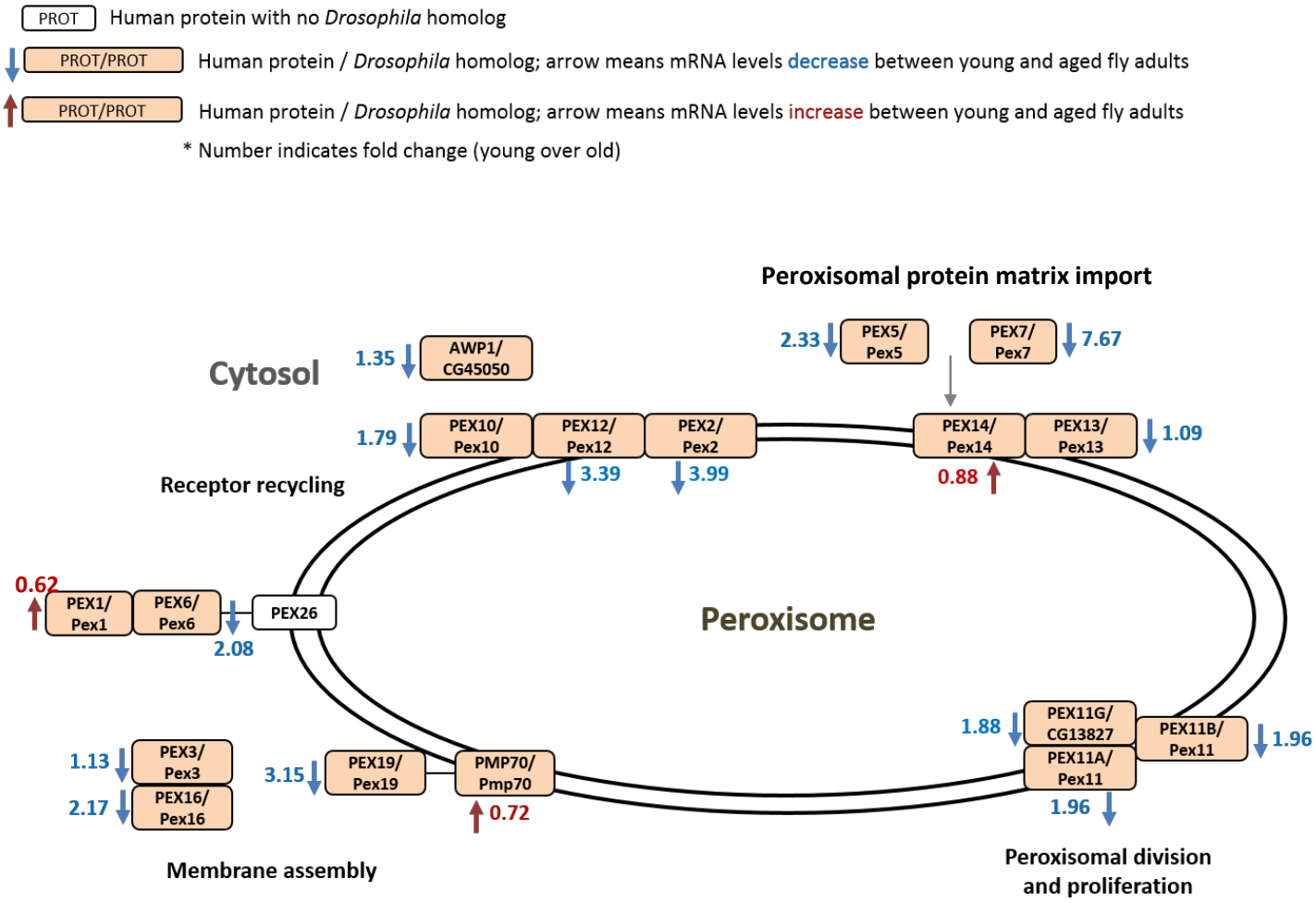

B

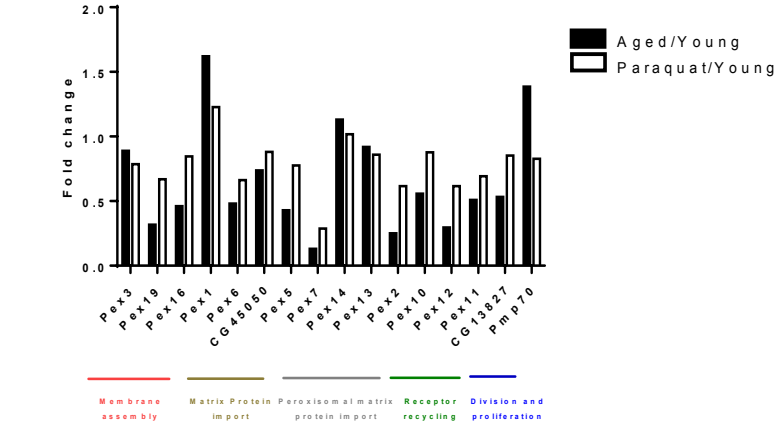

C

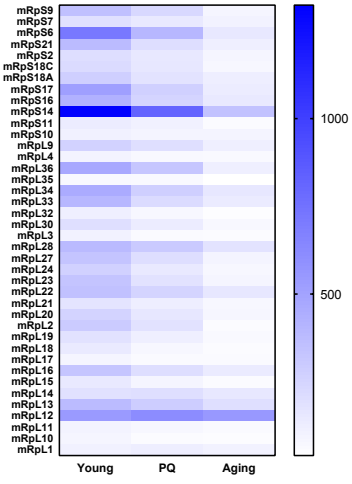

Figure 5

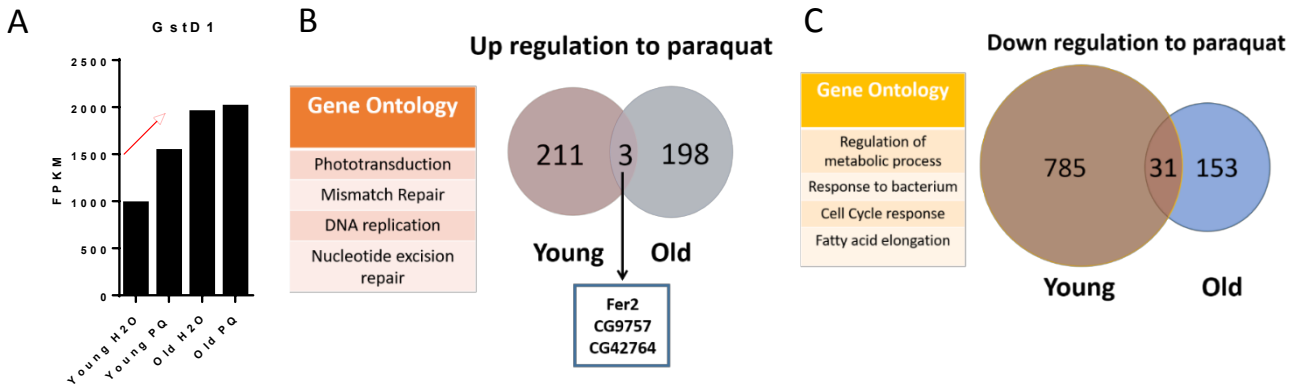

Figure 6

A

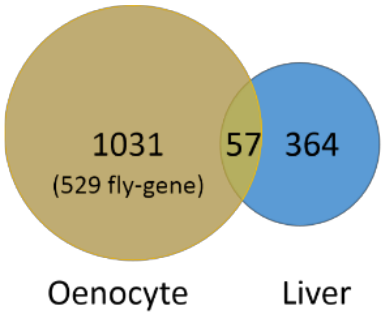

B

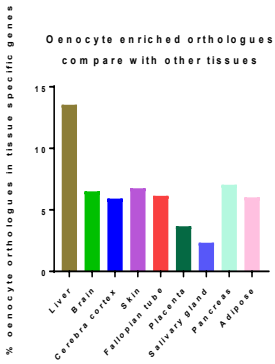

C

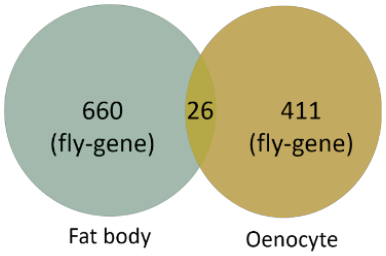

D

Fat body function	Oenocyte function
Biosynthesis of antibiotics	Proteasome
Biosynthesis of amino acids	Biosynthesis of unsaturated fatty acids
Fatty acid degradation	Synthesis and degradation of ketone bodies
Lysosome	Xenobiotics by cytochrome P450

E

F

	Gene symbol
Glucose Metabolism	PKLR
	DCXR
Ketogenesis	HMGCS2
Acyl-CoA ligase activity	ACSM3
	ACSM2B
	ACSM5
	ACSM2A
Ethanol metabolism	ADH1B
	ADH4
	ADH1A
	ADH1C
	ADH6
Fatty acid metabolism	ELOVL2
FGF family	FGF21
Lectin-like receptor	CLEC1B
	CLEC4M

G

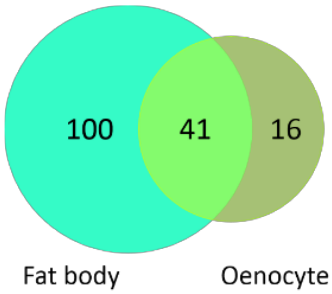

H

KEGG pathway of fat body enriched genes
Complement and coagulation cascades
Steroid hormone biosynthesis
Ascorbate and aldarate metabolism
Drug metabolism
Retinol metabolism
Pentose and glucuronate interconversions
Porphyrin and chlorophyll metabolism
Glycan biosynthesis and metabolism
Chemical carcinogenesis
Glycine, serine and threonine metabolism
Staphylococcus aureus infection

I

KEGG pathway of shared liver orthologue
Retinol metabolism
Metabolism of xenobiotics by cytochrome P450
Linoleic acid metabolism
Steroid hormone biosynthesis
Bile secretion

Figure 7

A

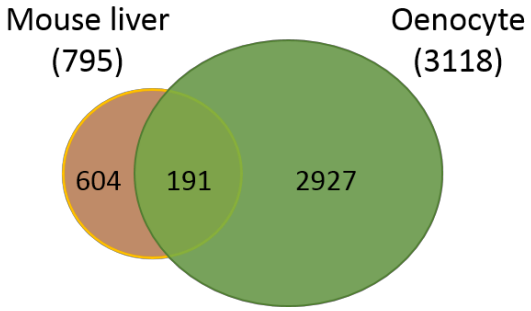

Drug and xenobiotics metabolism:
Including CYP3A fly ortholog Cyp6a8.
MAPK cascade and NF-kappaB increase:
To confer increased oxidative stress
DNA double-strand break repair
Transport of glucose, bile salts and organic acids
Decreased bile salt secretion in old liver
Insulin signaling:
Age related changes in liver insulin signaling

B

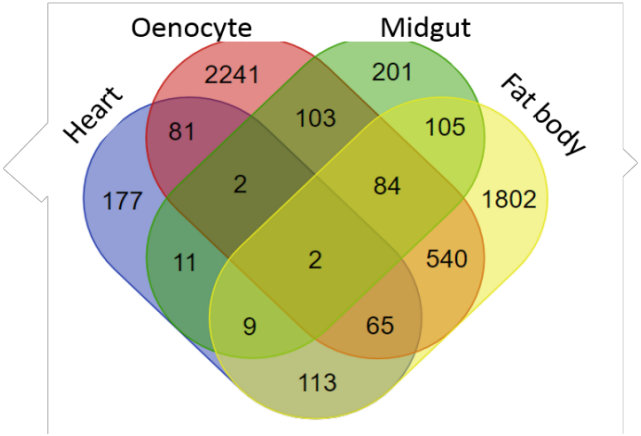

Oenocyte	Midgut	Fat body	Heart
Ribosome structure	Transporter activity	RNA metabolism	Phosphatidylinositol
Insulin receptor cascade	DNA replication	Drug metabolism	Phagosome
Peroxisome (mainly found in liver)	Glycan degradation	Metabolic pathway	Lysosome
Mitochondrial protein synthesis		Membrane trafficking	Actin cytoskeleton

Table 1: GSEA analysis revealed age-related decreases in oenocyte mitochondrial and peroxisome function, and increases in DNA repair.

Pathways Enriched in Young Flies

NAME	NOM p-val	FDR q-val
PROTEASOME	0.000	0.002
RIBOSOME	0.000	0.001
OXIDATIVE PHOSPHORYLATION	0.000	0.001
THIAMINE METABOLISM	0.000	0.008
CARBON METABOLISM	0.000	0.007
PEROXISOME	0.000	0.008
GALACTOSE METABOLISM	0.000	0.016
NEUROACTIVE LIGAND-RECEPTOR INTERACTION	0.001	0.015
GLYCOLYSIS / GLUCONEOGENESIS	0.004	0.033
PENTOSE PHOSPHATE PATHWAY	0.006	0.013
LYSOSOME	0.006	0.089
FATTY ACID METABOLISM	0.007	0.033
FATTY ACID ELONGATION	0.018	0.049
GLYOXYLATE AND DICARBOXYLATE METABOLISM	0.018	0.044
GLYCINE, SERINE AND THREONINE METABOLISM	0.019	0.045

Pathways Enriched in Paraquat-treated Flies

NAME	NOM p-val	FDR q-val
DNA REPLICATION	0.000	0.003
MISMATCH REPAIR	0.000	0.003
BASE EXCISION REPAIR	0.006	0.029
NUCLEOTIDE EXCISION REPAIR	0.000	0.011
FANCONI ANEMIA PATHWAY	0.000	0.043

Pathways Enriched in Old Flies

NAME	NOM p-val	FDR q-val
DNA REPLICATION	0.000	0.028
MISMATCH REPAIR	0.000	0.025
BASE EXCISION REPAIR	0.012	0.035
UBIQUITIN MEDIATED PROTEOLYSIS	0.000	0.078
ENDOCYTOSIS	0.000	0.110
FANCONI ANEMIA PATHWAY	0.004	0.039
NUCLEOTIDE EXCISION REPAIR	0.008	0.037
HIPPO SIGNALING PATHWAY 1	0.009	0.134
HOMOLOGOUS RECOMBINATION	0.014	0.067
APOPTOSIS 2	0.027	0.197

Pathways Enriched in Paraquat-treated Flies

NAME	NOM p-val	FDR q-val
PROTEASOME	0.000	0.111
LYSOSOME	0.001	0.094
OXIDATIVE PHOSPHORYLATION	0.001	0.123
PEROXISOME	0.001	0.199
FATTY ACID METABOLISM	0.009	0.175
FATTY ACID ELONGATION	0.018	0.152
NEUROACTIVE LIGAND-RECEPTOR INTERACTION	0.026	0.180
NITROGEN METABOLISM	0.036	0.201

Table 2: Identification of oenocyte-unique genes. 17 gene are uniquely expressed in oenocyte compared to Flyatlas 1 and Flyatalas 2 databases.

CG33156	NAD kinase. Required for the antioxidant activities, oxidative phosphorylation
Notum	An enzyme that cleaves Glycophosphatidylinositol (GPI) anchors. Involved in Wnt signaling regulation.
CG13679	-
Oseg5	Outer segment 5
CG8736	Structural constituent of cuticle
CG14770	-
CG13047	Lethal, pain response defective
CG14515	Homologous to ferric-chelate reductase, members of cytochrome b561.
CG34214	Human homologue RBM28 protein is a specific nucleolar component of the spliceosomal snRNPs
CG14422	-
CG5386	Contains WD40.
CG12836	-
CG15766	Agmatine N-acetyltransferase. N-acetyltransferase
CG14257	-
TwdlZ	TweedleZ, strucural constituent of chitin-based cuticle
TwdlN	TweedleN, strucural constituent of chitin-based cuticle
Ccp84Ae	Ccp84Ae, structural constituent of cuticle